

**PHYSICAL MODEL SIMULATION OF PLANE SLIDING
FAILURE OF JOINTED ROCK SLOPE**

Matsee Kleepmek



A Thesis Submitted in Partial Fulfillment of the Requirements for the

Degree of Master of Engineering in Geotechnology

Suranaree University of Technology

Academic Year 2011

การจำลองการพังทลายแบบแผ่นระนาบของมวลหินที่มีรอยแตกบนความ
ลาดชันด้วยแบบจำลองทางกายภาพ



วิทยานิพนธ์นี้เป็นส่วนหนึ่งของการศึกษาตามหลักสูตรปริญญาวิศวกรรมศาสตรมหาบัณฑิต
สาขาวิชาเทคโนโลยีธรณี
มหาวิทยาลัยเทคโนโลยีสุรนารี
ปีการศึกษา 2554

**PHYSICAL MODEL SIMULATION OF PLANE SLIDING
FAILURE OF JOINTED ROCK SLOPE**

Suranaree University of Technology has approved this thesis submitted in partial fulfillment of the requirements for a Master's Degree.

Thesis Examining Committee

(Assoc. Prof. Kriangkrai Trisarn)

Chairperson

(Assoc. Prof. Dr. Kittitep Fuenkajorn)

Member (Thesis Advisor)

(Dr. Prachya Tepnarong)

Member

(Prof. Dr. Sukit Limpijumnong)

Vice Rector for Academic Affairs

(Assoc. Prof. Ft. Lt. Dr. Kontom Chamniprasart)

Dean of Institute of Engineering

มัทรี กลีบเมฆ : การจำลองการพังทลายแบบแผ่นระนาบของมวลหินที่มีรอยแตกบนความลาดชันด้วยแบบจำลองทางกายภาพ (PHYSICAL MODEL SIMULATION OF PLANE SLIDING FAILURE OF JOINTED ROCK SLOPE). อาจารย์ที่ปรึกษา : รองศาสตราจารย์ ดร. กิตติเทพ เฟื่องขจร, 80 หน้า.

วัตถุประสงค์ของการศึกษานี้คือเพื่อจำลองการพังทลายแบบแผ่นระนาบของความลาดชันที่ประกอบด้วยมวลหินที่มีรอยแตก โดยใช้แบบจำลองเชิงกายภาพแบบย่อส่วนในห้องปฏิบัติการ ผลการศึกษาสามารถช่วยให้เข้าใจเกี่ยวกับการเคลื่อนตัวของมวลหินในระหว่างการพังทลายแบบจำลองของความลาดชันถูกจัดเรียงโดยใช้หินทรายรูปสี่เหลี่ยมผืนผ้า และรูปสี่เหลี่ยมขนมเปียกปูนที่มีขนาด 4×4×8 ซม. 4×4×12 ซม. และ 4×4×16 ซม. ตัวอย่างหินบางก้อนถูกจัดเตรียมให้มีมุมด้านข้างเท่ากับ 45 องศา และ 135 องศา ผลกระทบของระยะห่างระหว่างรอยแตกและมุมของรอยแตกต่อเสถียรภาพของความลาดชันได้ถูกศึกษาในงานวิจัยนี้ ผลการทดสอบระบุว่า การพังทลายแบบแผ่นระนาบจะเกิดขึ้นสำหรับความลาดชันที่มีความเอียงและความสูงน้อยและมีระยะห่างระหว่างรอยแตกมาก การพังทลายแบบผสมระหว่างรูปโค้งและแผ่นระนาบจะเกิดขึ้นเมื่อความลาดชันมีความเอียงและความสูงมากและมีระยะห่างระหว่างรอยแตกน้อย ความสูงของความลาดชันที่มากที่สุดจะลดลงถ้ามุมของการเคลื่อนไหลและมุมของหน้าลาดเอียงมีค่าสูงขึ้น แบบจำลองความลาดชันที่มีทิศทางของรอยแตกเอียงเข้าไปด้านในจะมีเสถียรภาพน้อยกว่าความลาดชันที่มีรอยแตกเอียงออกมาทางด้านหน้า ผลจากแบบจำลองทางกายภาพสอดคล้องเป็นอย่างดีกับผลที่ได้จากการคำนวณด้วยระเบียบวิธีเชิงตัวเลข สูตรสำเร็จของ Hoek and Bray จะประเมินค่าเสถียรภาพของแบบจำลองเชิงกายภาพสูงเกินความเป็นจริง ในขณะที่สูตรสำเร็จของ Bishop จะประเมินค่าเสถียรภาพของแบบจำลองเชิงกายภาพต่ำกว่าความเป็นจริงในทุกกรณี

MATSEE KLEEMK : PHYSICAL MODEL SIMULATION OF PLANE
SLIDING FAILURE OF JOINTED ROCK SLOPE. THESIS ADVISOR :
ASSOC. PROF. KITTITEP FUENKAJORN, Ph.D., P.E., 80 PP.

PLANE FAILURE/FRICTION/ /PHYSICAL MODEL/ CYCLIC LOAD

The objective of this study is to simulate plane sliding failures in jointed rock slopes using scaled-down physical model in the laboratory. The results can help understanding the rock mass movement during failure. The slope models are formed by rectangular and parallelepiped blocks of sandstone with nominal sizes of 4×4×8 cm, 4×4×12 cm, and 4×4×16 cm. Some blocks are prepared to obtain parallelogram shape with angles of 45° and 135°. The effects of joint spacing and joint intersection angles on the stability of the rock slopes have been studied. Results indicate that plane sliding occurs when the slopes are gentle and low with large joint spacing while combination of circular and plane sliding modes is observed when the slopes are steep and high with small joint spacing. The maximum slope height also decreases as the sliding plane angle and slope face angle increase. The slope models with joint dipping into the slope face tend to be less stable than those with the joint dipping away from the slope face. The simulation results well agree with those of the UDEC analyses. Hoek and Bray's solution severely overestimate the stability of the slope models, the simplified Bishop method underestimate the stability of the slope models for all joint conditions.

School of Geotechnology

Academic Year 2011

Student's Signature_____

Advisor's Signature_____

ACKNOWLEDGMENTS

I wish to acknowledge the funding support of Suranaree University of Technology (SUT).

I would like to express my sincere thanks to Assoc. Prof. Dr. Kittitep Fuenkajorn, thesis advisor, who gave a critical review and constant encouragement throughout the course of this research. Further appreciation is extended to Asst. Prof. Kriangkrai Trisarn: Chairman, School of Geotechnology and Dr. Prachya Tepnarong, School of Geotechnology, Suranaree University of Technology who are member of my examination committee. Grateful thanks are given to all staffs of Geomechanics Research Unit, Institute of Engineering who supported my work.

Finally, I most gratefully acknowledge my parents and friends for all their supported throughout the period of this research.

Matsee Kleepmek

TABLE OF CONTENTS

	Page
ABSTRACT (THAI).....	I
ABSTRACT (ENGLISH).....	II
ACKNOWLEDGEMENTS.....	III
TABLE OF CONTENTS.....	IV
LIST OF TABLES.....	VII
LIST OF FIGURES.....	VIII
SYMBOLS AND ABBREVIATIONS.....	X
CHAPTER	
I INTRODUCTION.....	1
1.1 Background of problems and significance of the study.....	1
1.2 Research objectives.....	1
1.3 Research methodology.....	2
1.3.1 Literature review.....	2
1.3.2 Sample preparation.....	2
1.3.3 Deterministic methods.....	4
1.3.4 Computer modeling.....	4
1.3.5 Physical model testing.....	4
1.3.6 Comparisons.....	4
1.3.7 Conclusions and thesis writing.....	4

TABLE OF CONTENTS (Continued)

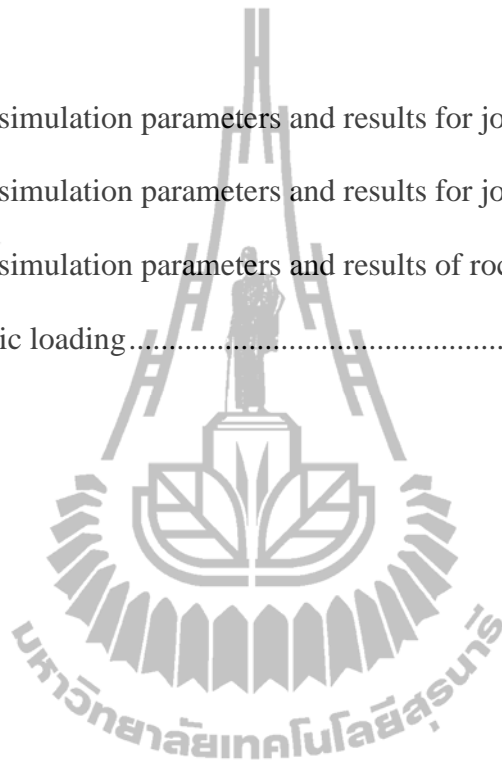
	Page
1.4 Scope and limitations of the study	5
1.5 Thesis contents	6
II LITERATUREREVIEW	7
2.1 Introduction.....	7
2.2 Plane sliding failure	7
2.3 Rock joints movement	11
2.4 Effect of seismic load.....	12
2.5 Physical models and numerical simulation.....	16
III TEST PLATFORM AND SAMPLE PREPARATION	22
3.1 Introduction.....	22
3.2 Design requirements and components	22
3.3 Rock samples	25
IV SLOPE MODEL SIMULATION.....	27
4.1 Introduction.....	27
4.2 Assessment of the joint spacing effects under static condition....	27
4.3 Assessment of the joint angle effects under static condition	32
4.4 Assessment of the joint spacing effects under dynamic loading ...	36
V DETREMINISTIC METHODS AND NUMERICAL ANALSIS	39
5.1 Introduction.....	39

TABLE OF CONTENTS (Continued)

	Page
5.2 Deterministic methods for joint spacing effects under static condition	39
5.2.1 Hoek and Bray's solution	39
5.2.2 Simplified Bishop method	41
5.3 Deterministic methods for joint angle effects under static condition	44
5.4 Deterministic methods for joint spacing effects under dynamic loading	45
5.5 Numerical analysis of joint spacing effects	48
5.6 Numerical analysis of joint angle effects	50
 VI DISCUSSIONS, CONCLUSIONS, AND RECOMMENDATIONS FOR FUTURE STUDIES	 53
6.1 Discussions	53
6.2 Conclusions	54
6.2 Recommendations for future studies	56
REFERENCES	57
APPENDICE	
APPENDIX A PUBLICATIONS	59
BIOGRAPHY	80

LIST OF TABLES

Table	Page
4.1 Summary of simulation parameters and results for joint spacing effects	30
4.2 Summary of simulation parameters and results for joint angle effect	34
4.3 Summary of simulation parameters and results of rock slope stability analysis under dynamic loading	37



LIST OF FIGURES

Figure		Page
1.1	Research plan.....	3
2.1	Geometry of slope exhibiting plane failure	9
2.2	Geometries of plane failure.....	10
2.3	Example of test arrangement	17
2.4	Shake table test apparatus for model slope.....	18
2.5	Experimental failure model of rock slope with difference joint structures and DEM simulations.....	19
2.6	Types of loading in different model experiments.....	21
3.1	Test frame used in physical model simulation.....	23
3.2	Crank arm and flywheel used to induce dynamic loading to the test platform	24
3.3	Sandstone rectangular blocks	26
3.4	Parallelogram shaped blocks.....	26
4.1	Joint spacing ratios ($S_H:S_V$).....	29
4.2	Some test results for $S_H:S_V = 1:2$ of combination failure mode	31
4.3	Some test results for $S_H:S_V = 1:3$ of plane failure mode.....	31
4.4	Some test results for $S_H:S_V = 1:4$ of plane failure mode.....	31
4.5	Simulation results for $S_H: S_V = 1:2, S_H: S_V = 1:3 S_H: S_V = 1:4$	32
4.6	Joint intersection angles and slope face angle (ψ_f)	33
4.7	Some test results for joint set with 45° intersections of plane failure mode....	34

LIST OF FIGURES (Continued)

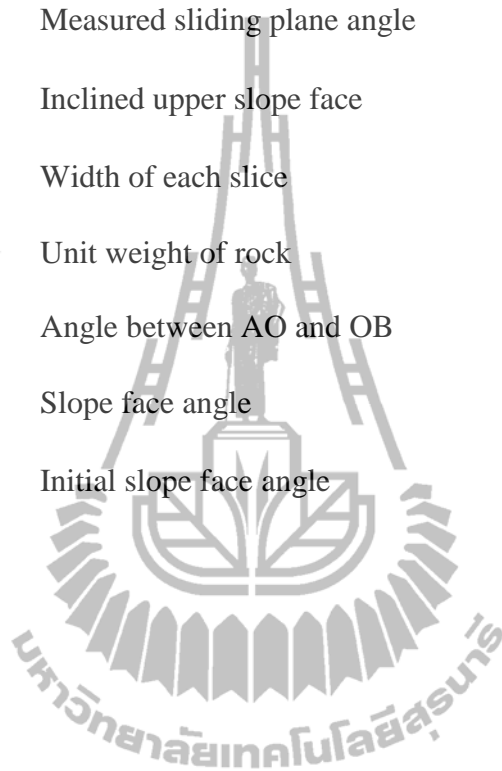
Figure	Page
4.8	Some test results for joint set with 135° intersections of plane failure mode 34
4.9	Simulation results for joint set with 45°, 90° and 135° intersections 35
4.10	Simulation results for $S_H: S_V = 1:2, 1:3$ and $1:4$ under dynamic loading 38
5.1	Parameters used for calculating the safety factor of a circular failure of simplified Bishop method 42
5.2	Comparisons between test results and deterministic methods for plane sliding mode and combination mode 43
5.3	Comparisons between test results and simplified Bishop solution for combination mode of failure 44
5.4	Comparisons between test results and deterministic method for various pseudo-static acceleration (a) 47
5.5	Comparisons between test results and UDEC analysis 49
5.6	Comparisons of test observations with UDEC simulations 50
5.7	Comparisons between test results and UDEC analysis 51
5.8	Test simulation and UDC result for joint set with 45° intersections 51
5.9	Test simulation and UDC result for joint set with 135° intersections 52

SYMBOLS AND ABBREVIATIONS

A	=	Contact area of sliding surface
a	=	Horizontal pseudo-static acceleration
b	=	Tension crack location measured from the slope crest
c	=	Cohesion of rock surface
FS	=	Factor of safety
h	=	Distance between the base and slope top
H	=	Slope height
R	=	Radius of wheel
S _H	=	Horizontal joints of the spacing
S _V	=	Vertical joints of the spacing
T	=	Duration of flywheel rotation
W	=	Weight of sliding block
y	=	Length of crack arm
z	=	Vertical tension crack depth
ϕ	=	Friction angle
ω_{AB}	=	Angular velocity of AB
α_{AB}	=	Relationship between the acceleration of points A and B
ω_{AB}	=	Angular velocity of AB
ψ_b	=	Base angle
ω_{OA}	=	Angular velocity of OA

SYMBOLS AND ABBREVIATIONS (Continued)

ω_{OA}	=	Angular velocity of OA
ψ_p	=	Measured sliding plane angle
ψ_s	=	Inclined upper slope face
Δx	=	Width of each slice
γ_r	=	Unit weight of rock
θ	=	Angle between AO and OB
ψ_f	=	Slope face angle
ψ_{f0}	=	Initial slope face angle



CHAPTER I

INTRODUCTION

1.1 Background of problems and significance of the study

The rock mass failure is a problem that can sometimes occur in the instability of rock slope area. It can cause damage to life and surface structures. The effects of joint spacing, joint angle, slope height and seismic loading are one of the important parameters for the design and stability analysis of the rock slopes. Scaled-down physical models have been used to simulate the failure behavior of rock slope in the laboratory which can help understanding the rock mass movement during failure. It has been used as teaching and research tools to reveal the two-dimensional failure process of rock slopes under various geological characteristics. The results from physical model simulation can also be used to compare with those obtained from the deterministic method and from the numerical methods. The comparisons can also assess the performance of the deterministic method and the computer modeling.

1.2 Research objectives

The objective of this study is to simulate the plane sliding failure using scaled-down physical model in the laboratory. The effects of joint spacing, joint angle and slope height are studied and compared the results with those obtained from the deterministic method and the numerical simulations.

1.3 Research methodology

This research consists of five main tasks; literature review, sample preparation, comparisons the physical model testing with deterministic method and computer simulation, conclusions and discussions and thesis writing and presentation. The work plan is illustrated in the Figure 1.1.

1.3.1 Literature review

Literature review has been carried out to study the rock slope failure criterion, and to study the results and factors of rock slope failure in particularly factors of earthquake vibration. The sources of information are from journals, technical reports and conference papers. A summary of the literature review has been given in the thesis.

1.3.2 Sample preparation

Phu Phan sandstone from Nakhon Ratchasima province has been selected for use as rock samples primarily because it has highly uniform texture, density and strength. To form slope models with two mutually perpendicular joint sets, rectangular shaped blocks have been prepared by 4×4×8 cm, 4×4×12 cm and 4×4×16 cm ($S_H : S_V$ ratios from 1:2, 1:3 to 1:4) blocks sizes. Some blocks are also prepared to simulate joint sets with 45 degrees and 135 degrees by parallelogram shaped blocks with dimensions of 4×4×8 cm ($S_H : S_V$ ratios 1:3). A total of nearly 1000 blocks of Phu Phan sandstone has been prepared.

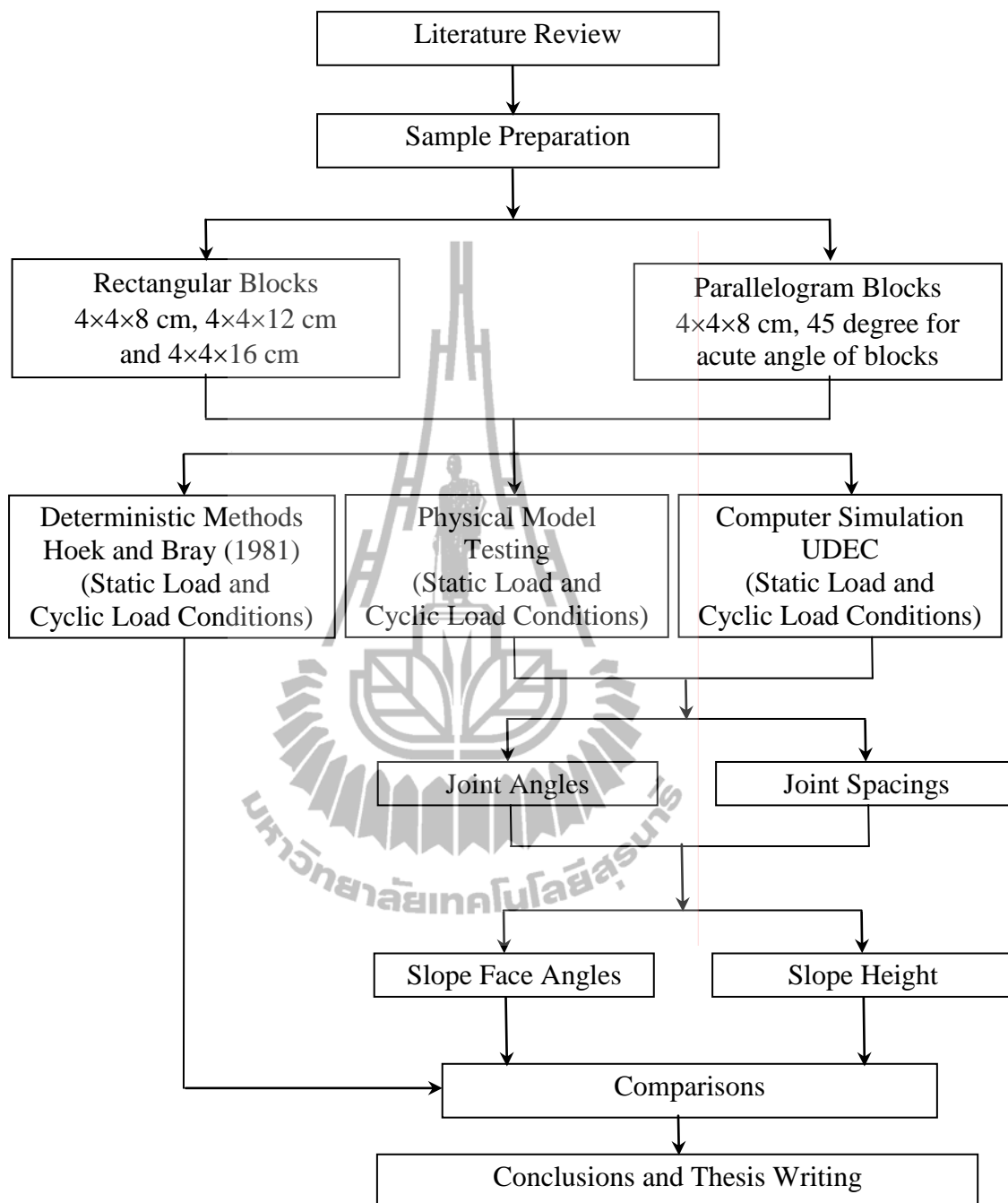


Figure 1.1 Research plan

1.3.3 Deterministic methods

The deterministic method given by Hoek and Bray (1981) is used to calculate the slope face angle (ψ_f) that causes failure. The variable involved in the testing is the slope face angle (ψ_f) at several slope heights.

1.3.4 Computer modeling

Slope face angle (ψ_f), joints spacing and slope height (H) have been used as variables in the numerical simulations with UDEC code. The testing includes the static load condition and cyclic load condition.

1.3.5 Physical model testing

Physical models are performed to simulate the failure of rock slope in the laboratory. The varied parameters are joint angle, joint spacing and slope height. They are performed under static loading condition and cyclic loading (lateral static acceleration) condition.

1.3.6 Comparisons

The results from the physical model simulation have been used to compare with the computer simulation results. Similarity and discrepancy are discussed.

1.3.7 Conclusions and thesis writing

All research activities, methods, and results have been documented and compiled in the thesis. The contents or findings have been published in the conference, proceedings or journals.

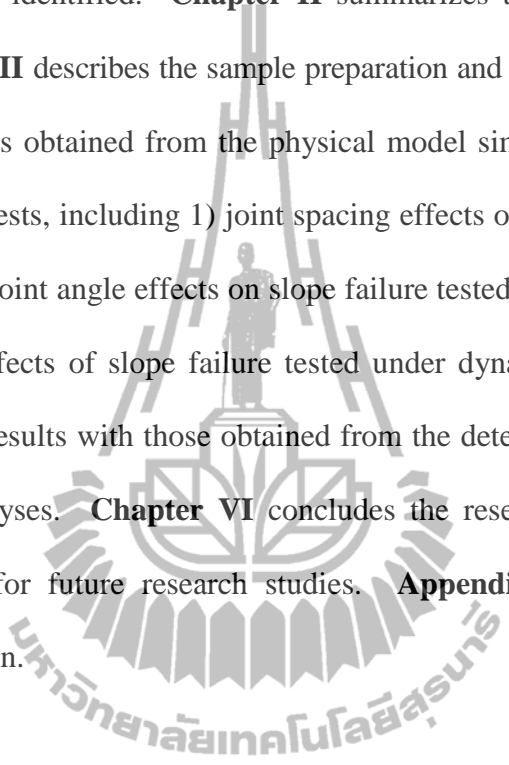
1.4 Scope and limitations of the study

The scope and limitations of the research include as follows.

- a. The test platform used in this study is designed by Pangpetch and Fuenkajorn (2007).
- b. The tests are Phu Phan sandstone as block specimens. The sandstone blocks prepared by saw-cutting are arranged to simulate rock slopes with two joint sets. The $S_H : S_V$ ratios vary from 1:2, 1:3 to 1:4 and to simulate joint sets with 45° and 135° angles.
- c. Slope height (H) varies from 0.08 m to slightly over 1 m.
- d. Failure of slope model is induced by using real gravitational force. There are two accelerations ranging from 0.09g to 0.21g.
- e. The physical model simulations are under dry conditions and clean joints
- f. Video camera and digital camera continuously record the slope movement for measurements of the slope angle and height immediately before failure.
- g. The observed results are compared with those calculated by the deterministic methods given by Hoek and Bray (1981), simplified Bishop (1995) and with the results from computer simulation using UDEC code.
- h. The tests are performance under static and cyclic loading.
- i. The research findings will be published in conference paper or journal.

1.5 Thesis contents

Chapter I introduces the thesis by briefly describing the background of problems and significance of the study. The research objectives, methodology, scope and limitations are identified. **Chapter II** summarizes the results of the literature review. **Chapter III** describes the sample preparation and test platform. **Chapter IV** describes the results obtained from the physical model simulation. The experiments are divided into 3 tests, including 1) joint spacing effects on slope failure tested under static condition 2) joint angle effects on slope failure tested under static condition, and 3) joint spacing effects of slope failure tested under dynamic loading. **Chapter V** compares the test results with those obtained from the deterministic method and from the numerical analyses. **Chapter VI** concludes the research results, and provides recommendations for future research studies. **Appendix A** provides detailed of technical publication.



CHAPTER II

LITERATURE REVIEW

2.1 Introduction

This chapter summarizes the results of literature review carried out to improve an understanding of the simulation of rock slope failure using physical model. The topics reviewed here include the plane sliding failure, rock joints movement, effect of seismic load, physical models and numerical simulations.

2.2 Plane sliding failure

A plane slide forms under gravity alone when a rock block rests on an inclined weakness plane that “daylights” into free space (Hoek and Bray, 1981; Goodman, 1989). The inclination of the plane of slip must be greater than the friction angle of that plane. The conditions for failure reside dormant in the slope until excavation or rock movement removes the barrier to block translation. Movement of a block supposes that the restraint to sliding has been overcome not only along the surface of sliding but along the lateral margins of the slide. In soft rocks, like shale, the side restraint can be released by rupture of the rock itself if the base of sliding is inclined considerably steeper than the friction angle. In hard rocks, plane sliding can occur only if there are other discontinuities or valleys transverse to the crest of the slope releasing the sides of the block (Hoek and Bray, 1981).

Wyllie and Mah (2004) described the general conditions for plane failure. In order for this type of failure to occur, the following geometrical conditions must be satisfied (Figure 2.1):

- a) The plane on which occurs must have strike parallel or nearly parallel (within approximately $\pm 20^\circ$) to the slope face.
- b) The sliding plane must “daylight” in the slope face, which means that the dip of the plane must be less than the dip of the slope face, that is $\psi_p < \psi_f$.
- c) The dip of the sliding plane must be greater than the angle of friction of this plane, that is $\psi_p > \phi$.
- d) The upper end of the sliding surface either intersects the upper slope, or terminates in a tension crack.
- e) Release surface that provide negligible resistance to sliding must be present in the rock mass to define the lateral boundaries of the slide. Alternatively, failure can occur on a sliding plane passing through the convex “nose” of a slope.

Using the shear strength parameters c and ϕ , the factor of safety (FS) of plane sliding given by the total force resisting sliding to the total force tending to induce sliding, is (Hoek and Bray, 1981):

$$FS = \left[cA + (W \cos \psi_p - U - V \sin \psi_p) \tan \phi \right] / W \sin \psi_p + V \cos \psi_p \quad (2.1)$$

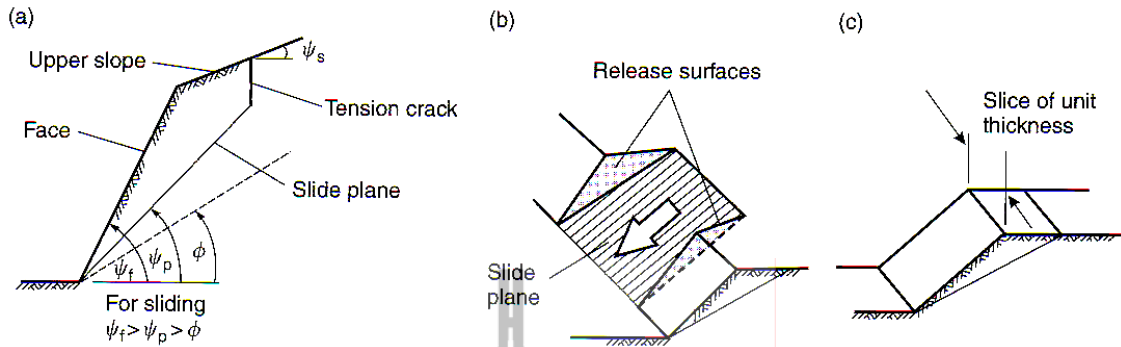


Figure 2.1 Geometry of slope exhibiting plane failure: (a) cross-section showing planes forming a plane failure; (b) release surface at ends of plane failure; (c) unit thickness slide used in stability analysis. (Wyllie and Mah, 2004)

where

$$A = (H - Z) \cos \psi_p \quad (2.2)$$

$$U = \frac{1}{2} \gamma_w Z_w (H - Z) \cos \psi_p \quad (2.3)$$

$$V = \frac{1}{2} \gamma_w Z_w^2 \quad (2.4)$$

for tension crack in the upper slope surface

$$W = \frac{1}{2} \gamma H^2 \left[\left(1 - (Z/H)^2 \right) \cot \psi_p - \cot \psi_f \right] \quad (2.5)$$

and, for the tension crack in the slope face

$$W = \frac{1}{2} \gamma H^2 \left[\left(1 - Z/H \right)^2 \cot \psi_p (\cot \psi_p \tan \psi_f - 1) \right] \quad (2.6)$$

where c is cohesive strength, ϕ is angle of friction, γ is unit weight of rock, γ_w is unit weight of water, A is area of face, H is slope height, W is weight of the sliding block, U is uplift water force, V is horizontal water force, Ψ_f is slope face angle, Ψ_p is sliding plane angle, Z_w is water depth, and Z is tension crack depth. When the tension crack is not vertical the above equations cannot be used and it is often easier to determine A , W , Z , and Z_w using a scale drawing on graph paper. The symbols mentioned are illustrated in Figure 2.2.

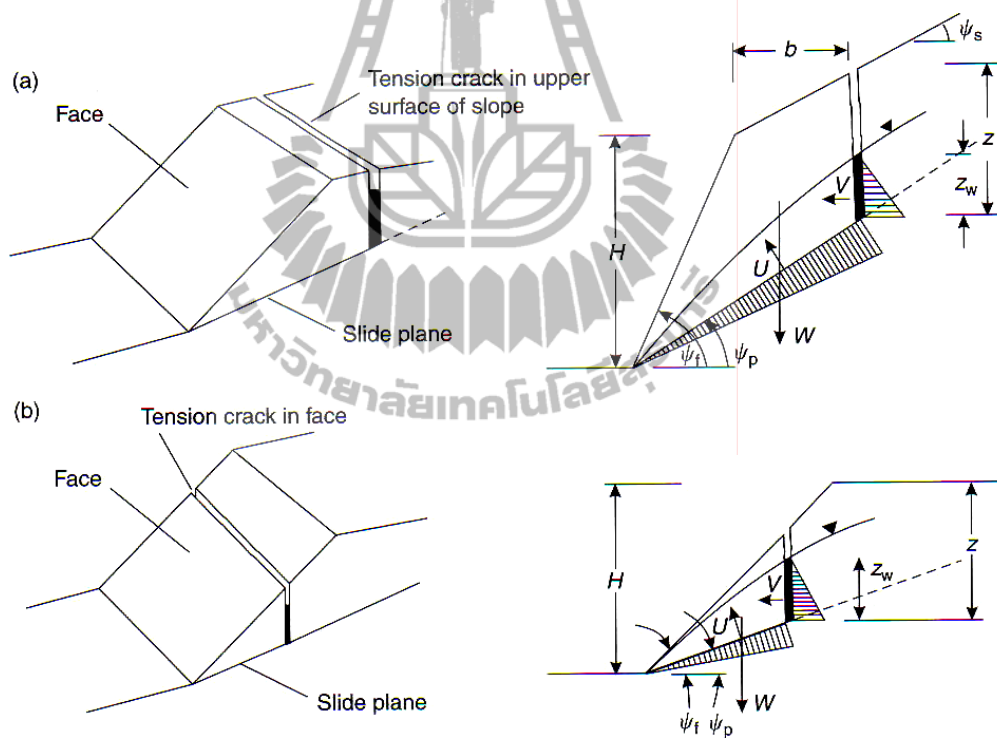


Figure 2.2 Geometries of plane failure: (a) tension crack in the upper slope; (b) tension crack in the face. (Wyllie and Mah, 2004)

2.3 Rock joints movement

The mechanical rock properties are one of the most important parameters that will be used in the analysis and design of any engineering in rock mass, particularly joint shear strength and basic friction angle. The standard of rock joint shear strength test methods as laboratory direct shear test and field direct shear test. Coulomb criterion represents the relationship between the peak shear strength and normal stress by costs include costs of sample maintain, transport, prepares, and testing.

$$\tau = c + \sigma_n \tan \phi \quad (2.7)$$

where τ is joint shear strength, σ_n is normal stress, c is the cohesive strength, and ϕ is angle of friction. These factors are the laboratory result. The result may be not agrees with rock mechanics work and high compressive strength. This is because of the relationship between τ and σ_n of Coulomb criterion is linear while actual relation is curve.

Patton (1966) performed a series of constant load stress direct shear tests with regular teeth inclination (i) at varying normal stresses. From these tests, he established a bilinear failure envelope – failure from an asperity sliding and asperity shearing mode.

$$\tau = \sigma_n \tan (\phi_B + i) \quad (2.8)$$

where τ is joint shear strength, σ_n is normal stress, ϕ_B is basic friction angle, and i is regular teeth inclination. Patton found that the inclination of the bedding plane trace was approximately equal to the sum of the average angle i and the basic friction angle

ϕ_B found from laboratory tests on planar surfaces. The discussion has been limited to the problem of shearing along a single discontinuity or along a family of parallel discontinuities and that the question of fracture of the material on either side of the discontinuities has not been considered. Fracturing of interlocking surface projections on rock discontinuities is an important factor which has to be considered when attempting to understand the behavior of actual rock surfaces.

Fairhurst's criterion;

$$\tau = \sigma_j \frac{\sqrt{(1+n)} - 1}{n} \left(1 + n \frac{\sigma}{\sigma_j} \right)^{\frac{1}{2}} \quad (2.9)$$

where σ_j is rock joint compressive stress and n is the compressive stress and tensile stress ratio of rock (σ_c/σ_T). Hoek (1968) has suggested that, for most hard rocks, n is approximately equal to 10.

Barton (1973) has studied the behavior of natural rock joints and proposed a criterion that is modified from Patton. It can be re-written as

$$\tau = \sigma_n \tan \{ \phi_B + JRC \log_{10} (\sigma_j / \sigma_n) \} \quad (2.10)$$

where τ is joint shear strength, ϕ_B is basic friction angle, σ_n is normal stress, JRC is the joint roughness coefficient, and JCS is the joint wall compressive strength.

2.4 Effect of seismic load

Siad (2003) considered gravity and inertial forces developed in the rock mass by the passage of seismic waves are the external forces. The rock mass is crossed by

two sets of fractures which are considered to be planar and persistent. The stability factor is very sensitive to variations of horizontal seismic coefficient. It is reduced due to seismic effect. However, the value flattens as friction angle of fracture increases.

Kramer (1996) states that the magnitudes of the pseudostatic acceleration should be related to the severity of the anticipated ground motion as selection of pseudostatic accelerations for design are not a simple matter. The horizontal pseudostatic force clearly decreases the factor of safety. It reduces the resisting force (for $\phi > 0$) and increases the driving force. The vertical pseudostatic force typically has less influence on the factor of safety since it reduces (or increases, depending on its direction) both the driving force and the resisting force. As a result, the effects of vertical accelerations are frequently neglected in pseudostatic analyses resolving the forces on the potential failure mass in a direction parallel to the failure surface,

$$FS = \frac{\text{resisting force}}{\text{driving force}} = \frac{cl_{ab} + [(W - F_v)\cos\beta - F_h \sin\beta]\tan\phi}{(W - F_v)\sin\beta + F_h \cos\beta} \quad (2.11)$$

where c and ϕ are the Mohr-Coulomb strength parameters that describe the shear strength on the failure plane, l_{ab} is the length of the failure plane, W is the weight of the failure mass, and F_h and F_v are the horizontal and vertical inertial forces which act through the centroid of the failure mass. The magnitudes of the pseudostatic forces are

$$F_h = \frac{a_h W}{g} = k_h W \quad (2.12)$$

$$F_v = \frac{a_v W}{g} = k_v W \quad (2.13)$$

where a_h and a_v are horizontal and vertical pseudostatic accelerations, k_h and k_v are dimensionless horizontal and vertical pseudostatic coefficients. Pseudostatic analyses can be unreliable for soils that build up large pore pressures or show more than about 15% degradation of strength due to earthquake shaking. The pseudostatic approach can be used to evaluate pseudostatic factors of safety for planar, circular, and noncircular failure surfaces. Many commercially available computer programs for limit equilibrium slope stability analysis have the option of performing pseudostatic analyses.

Hatzor et al. (2004) analyzed dynamic stability of jointed rock slopes using the dynamic discontinuous deformation analysis (DDA). Comparison of predicted damage with actual slope performance over a historic time span of 2000 years allows they concluded that introduction of 2% kinetic damping should suffice for realistic damage predictions. The peak horizontal ground acceleration (PGA) for DDA computation varied from 0.06g to 0.2g. The acceleration levels of 1g blocks at upper row in terrace may be expected to lift in the air for very short time spans when the scaled accelerations attain a level of 1g. It should be noted that the frequency content was not altered in the scaled records as all acceleration components were multiplied by a scalar only. It is not possible to check the validity of this result of DDA. The effect of bolting is apparent with the dense bolting pattern the terrace remains virtually intact after 10s of shaking with $PGA = 0.6 \text{ g}$.

Li et al. (2009) apply the finite element upper and lower bound techniques to this problem with the aim of providing seismic stability charts for rock slopes. These

chart solutions bound the true stability numbers within $\pm 9\%$ or better and are suited to isotropic and homogeneous intact rock or heavily jointed rock masses. A comparison of the stability numbers obtained by bounding methods and the limit equilibrium method has been performed where the latter was found to predict unconservative factors of safety for steeper slopes. These stability charts, including the earthquake effects, are based on the Hoek–Brown failure criterion and can be used for estimating seismic rock slope stability in the initial design phase. This study follows the general consideration of the earthquake effects which only takes the horizontal seismic coefficient (k_h) into account. A range of k_h magnitudes is also included, which are consistent with most design codes. Although the vertical seismic coefficient (k_v) is often ignored in practice, it is still worth investigating its influence on the stability of rock slopes in further studies.

Latha and Garaga (2010) study seismic slope stability of a rock slope in the Himalayan region of India is studied using pseudo-static and time response analysis in FLAC. The results obtained from the pseudo-static analysis are presented in the form of Factor of Safety (FS) and the results obtained from the time response analysis of the slope are presented in terms of horizontal and vertical displacements along the slope. The results obtained from both the analyses confirmed the global stability of the slope as the FS in case of pseudostatic analysis is above 1.0 and the displacements observed in case of time response analysis are within the permissible limits. The results obtained from the parametric analysis performed in the case of time response analysis in order to understand the effect of individual parameters on the overall stability of the slope. The displacements observed in the slope for the maximum credible earthquake in the region are well within the permissible limits. Peak

amplitude of the earthquake event has less influence on the seismic response of the slope as observed from the dynamic analyses carried out using three different earthquake scenarios. Pseudo-static analyses, where only peak amplitude alone is considered, will lead to erroneous results while predicting the deformations. Increase in the shear strength of rock mass reduces seismic deformations of the slope.

2.5 Physical models and numerical simulation

Pangpetch and Fuenkajorn (2007) used physical models or scaled-down models to simulate the failure behavior of rock slope in the laboratory. The design objectives are that it must be capable of simulating sliding and toppling failures under both dry and submerged conditions, and should allow assessing the effects of dynamic load (lateral static acceleration) on the slope stability. Figure 2.3 shows the test platform with block samples loaded inside the test frame. The simulation results indicate that the deterministic method of Hoek and Bray overestimates of plane sliding by as much as 30%. The observed toppling failures agree well with those determined by Hoek and Bray solution when the friction between blocks is considered in the calculation.

Pangpetch and Fuenkajorn (2009) study rock slope failure under static and dynamic loads. The failure is induced by true gravitational force and horizontal pseudo-static acceleration of up to 0.225 g. The effect of water-submerging is investigated. The comparisons of the test results with the deterministic solutions (by Hoek and Bray, 1981) and computer simulations (FLAC_Slope code) have revealed significant implications. Under static condition the deterministic method and computer simulation overestimate the factor of safety for the plane sliding failure by about 5 to

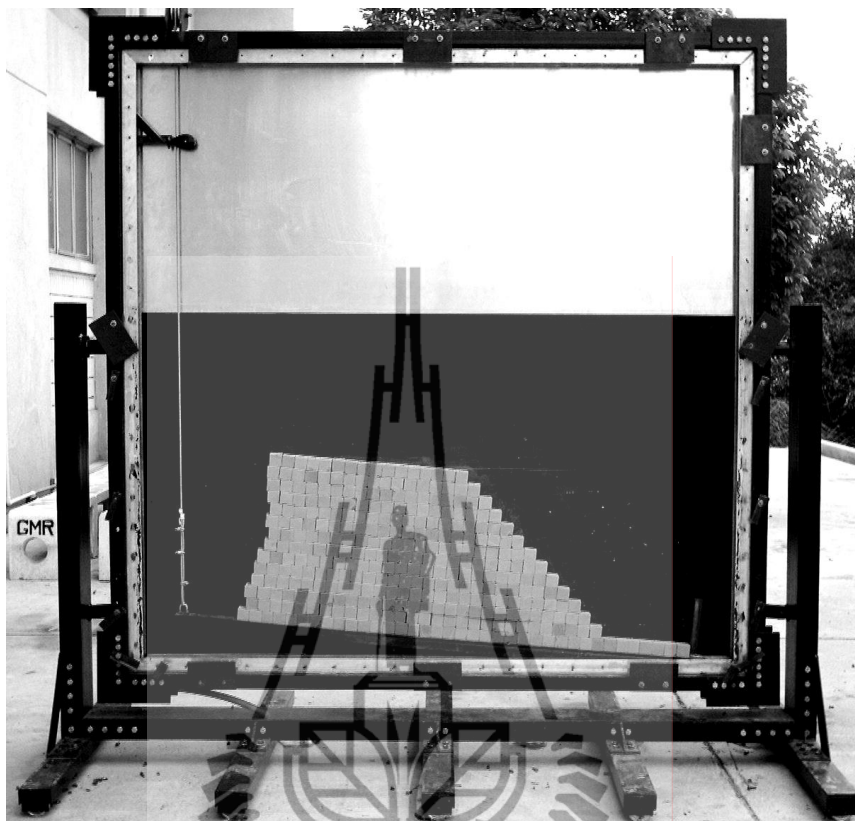


Figure 2.3 Example of test arrangement: Cubical blocks of Phu Phan sandstone placed in test platform (Pangpetch and Fuenkajorn, 2007).

10%, particularly for the slope models with shorter blocks. The discrepancy between the deterministic method and the test results under dynamic loading is highly significant. These findings indicate that under dynamic loading plane sliding analysis using the simple deterministic method for rock slopes with small joint spacing compared to the slope height will give a non-conservative result. In addition, the deterministic approach for stability analysis of low-angled sliding planes under under dynamic loading may be inappropriate.

Kokusho and Ishizawa (2005) studied the energy approach for earthquake induced slope failure evaluation by used shaking table (Figure 2.4). They proposed

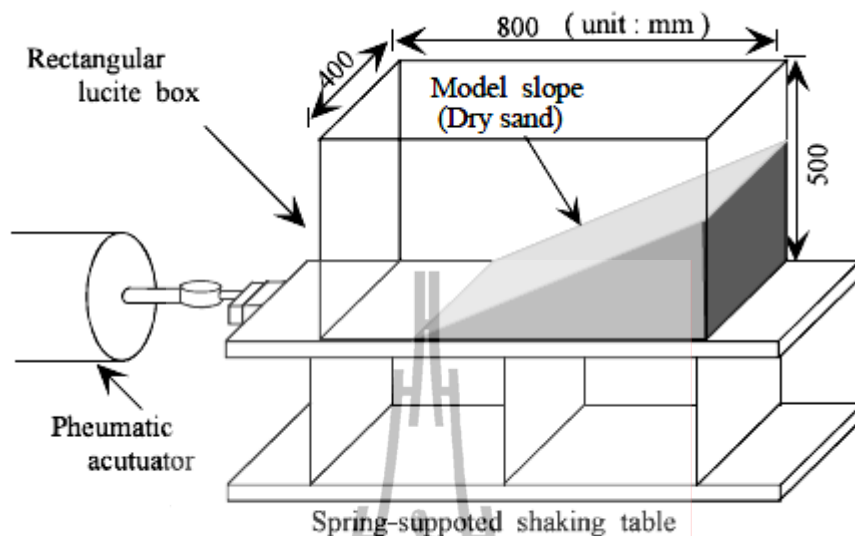


Figure 2.4 Shake table test apparatus for model slope (Kokusho and Ishizawa, 2005).

that the earthquake energy used for the slope failure can be successfully quantified in the test and its contribution to displacement is discussed in the light of the energy balance established for the block model.

Li et al. (2007) analyzed critical excavation depth for a jointed rock slope using a Face-to-Face Discrete Element Method (DEM) is illustrated in Figure 2.5. The DEM is based on the discontinuity analysis which can consider anisotropic and discontinuous deformations due to joints and their orientations. They compared the effect of joints on the failure modes between DEM simulations and experimental observations. It is found that the DEM predicts a lower critical excavation depth than the LEM (limit equilibrium method) of the joint structures in the rock mass are not ignored.

Roy and Mandal (2009) used sand model experiments this paper investigates failure mechanism of bed materials along hill slopes due to overburden loading. The

analysis takes into account three factors: 1) surface slope (α), 2) loading pattern and 3) mechanical anisotropy of bed materials. With progressive loading, the process of slope instability in sand models involves deformation localization in two modes:

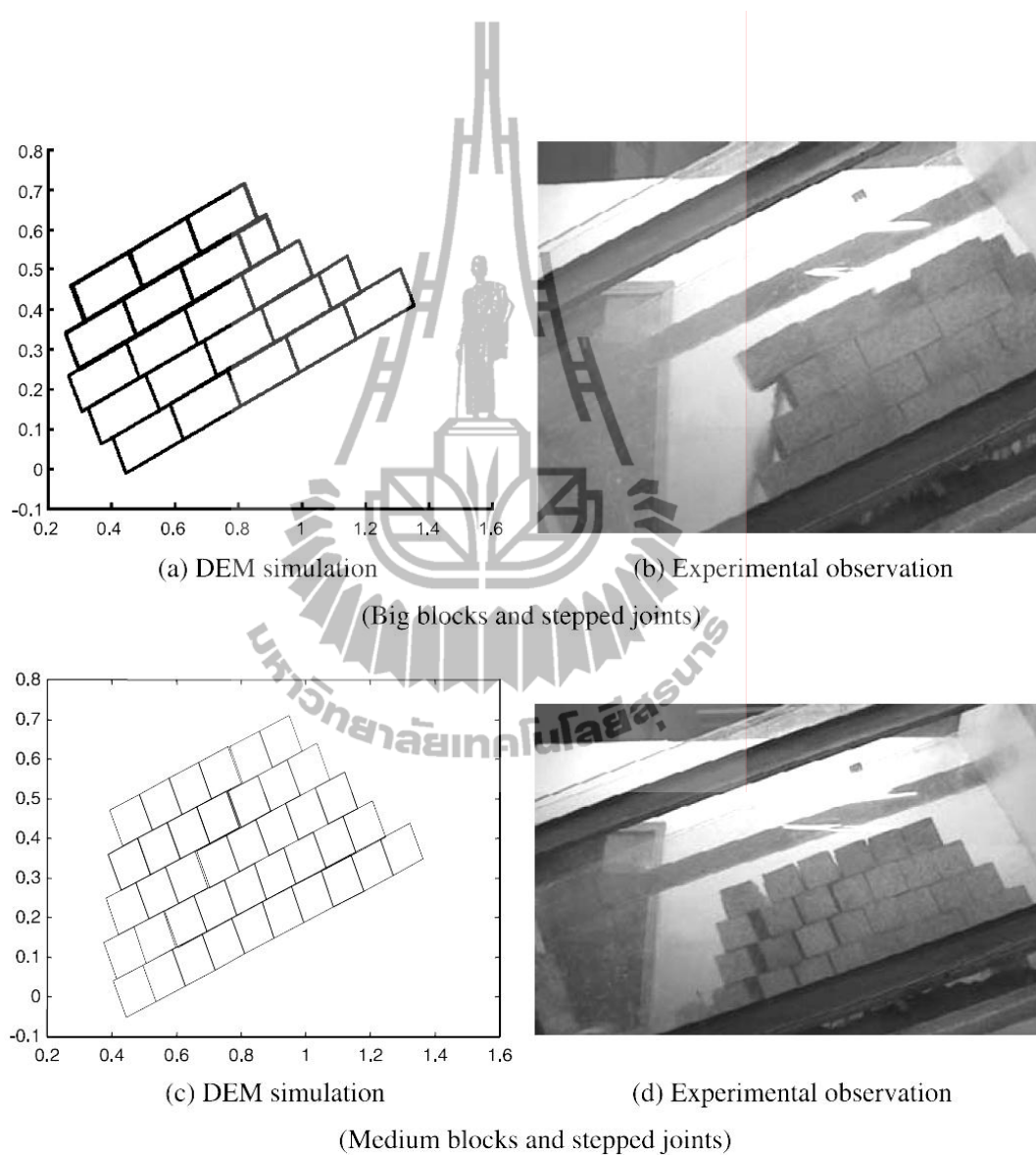
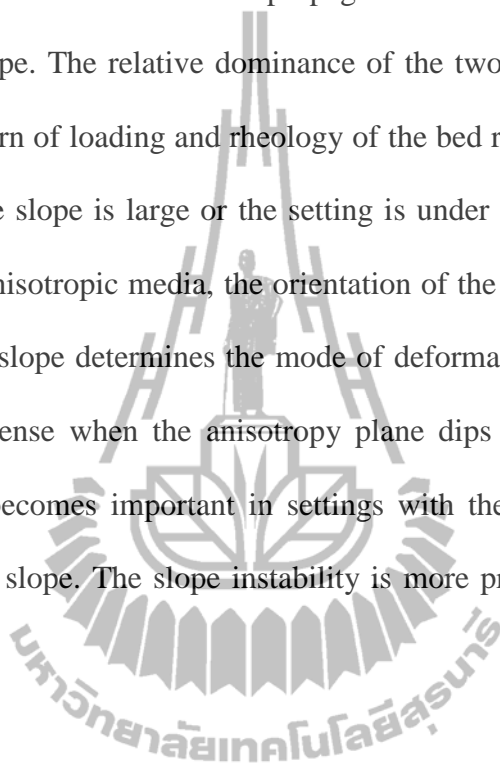


Figure 2.5 Experimental failure model of rock slope with difference joint structures and DEM simulations (Li et al., 2007).

compaction (Mode 1) and shear failure (Mode 2). The failure on natural slopes can be triggered due to deformation localization below civil or any geological overburden loads on the slopes. The process involves two contrasting modes are compaction and shear failure. The shear failure are propagates fast in the slope direction and destabilizes the slope. The relative dominance of the two modes is a function of the surface slope, pattern of loading and rheology of the bed rock. Mode 2 becomes more important when the slope is large or the setting is under loading with extended rigid block. In case of anisotropic media, the orientation of the anisotropy plane relative to that of the surface slope determines the mode of deformation localization. Mode 1 is relatively more intense when the anisotropy plane dips same as the surface slope, whereas Mode 2 becomes important in settings with the anisotropy planes dipping against the surface slope. The slope instability is more pronounced in the latter case (Figure 2.6).



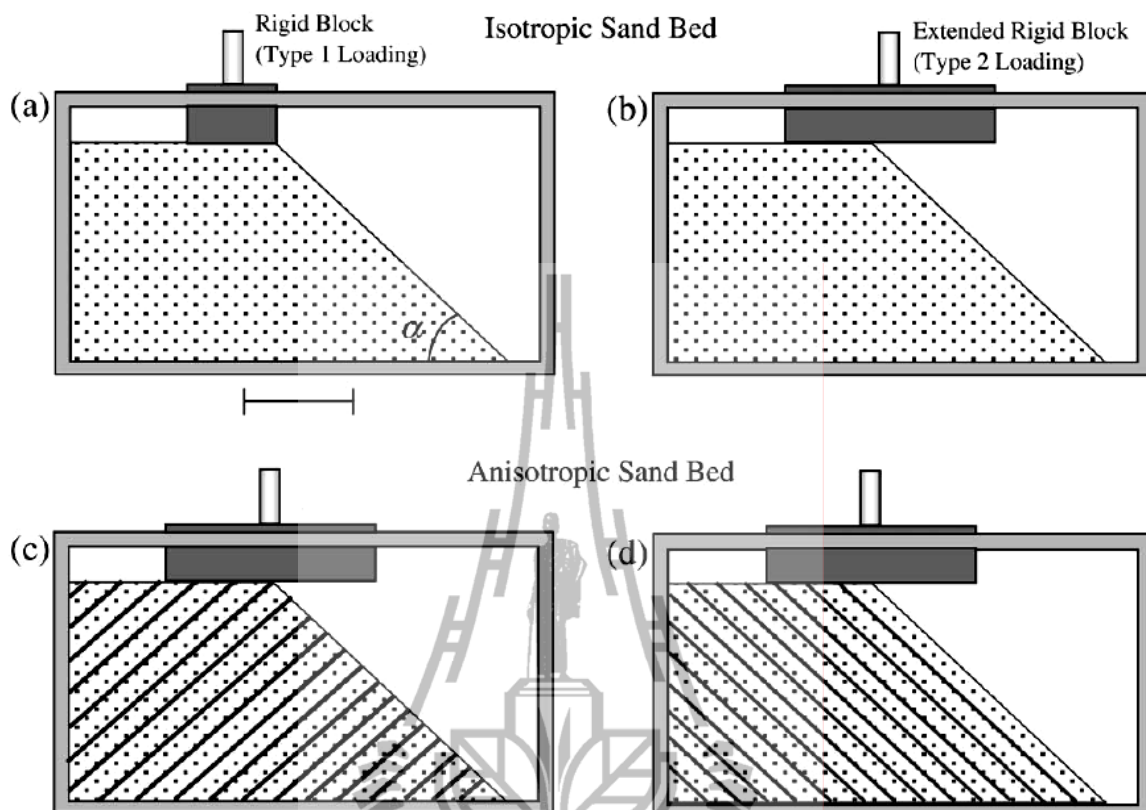


Figure 2.6 Types of loading in different model experiments: Type 1 loading with rigid block extended up to the model edge and Type 2 loading with rigid block extended beyond the model edge. (a) & (b) Isotropic sand models subjected to Type 1 and Type 2 loading respectively. (c) & (d) Anisotropic sand models subjected to Type 2 loading and the planes of anisotropy dipping against and towards the direction of surface slope (α) respectively. Scale bar: 10 cm (Roy and Mandal, 2009)

CHAPTER III

TEST PLATFORM AND SAMPLE PREPARATION

3.1 Introduction

This chapter describes the requirements and components of the test platform designed by Pangpetch and Fuenkajorn (2007). The device is used in this study. The preparation and specifications of the tested rock sample are also described in this chapter.

3.2 Design requirements and components

The test platform used in this study is designed by Pangpetch and Fuenkajorn (2007), as shown in Figure 3.1. The frame is hinged through steel rods in the middle to the stand allowing frame rotation from horizontal position during arranging and loading block samples to vertical position for testing under true gravitational force. When the frame is in horizontal position, the aluminum plate becomes a flat bed supporting the rock blocks during loading. The clear and removable acrylic sheet is installed before rotating the frame to the upright position to prevent the block samples from tipping over. It also allows visual inspection and monitoring of slope movement during the test. The test frame can accommodate 4 cm thick rock blocks arranged to a maximum height of up to 1.5 m to simulate two-dimensional jointed rock slopes.

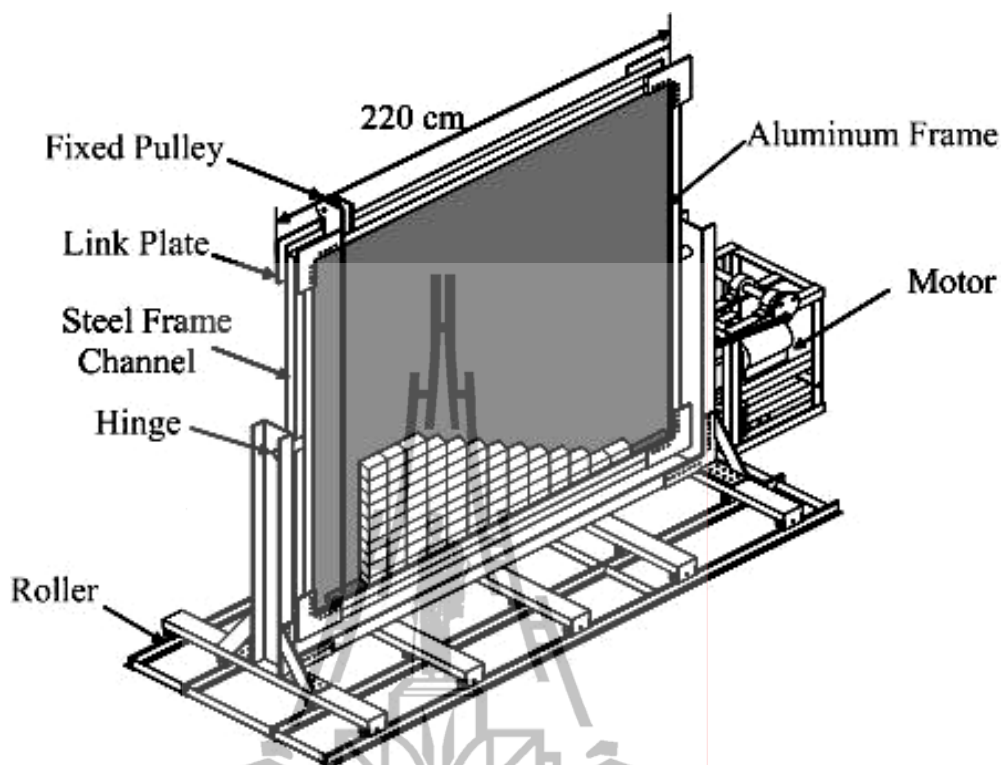


Figure 3.1 Test frame used in physical model simulation.

Steel grooved rollers mounted underneath the stand are used for testing under dynamic loading. The rollers will be placed on a set of steel rails equipped with a high torque motor, gear system and crank arm to induce a cyclic motion to the entire test platform. The frequency and amplitude of the horizontal pseudo-static acceleration can be controlled by adjusting the rotational diameter of the flywheel and speed of the motor.

Figure 3.2 shows the crank arm components used to generate the horizontal acceleration to the test frame. The acceleration at point B, represented by “a”, can be calculated using a set of equations given by Riley and Sturges (1993).

$$a = R\omega_{OA}^2 \cos \theta + y\omega_{AB}^2 \cos \phi - y\alpha_{AB} \sin \phi \quad (3.1)$$

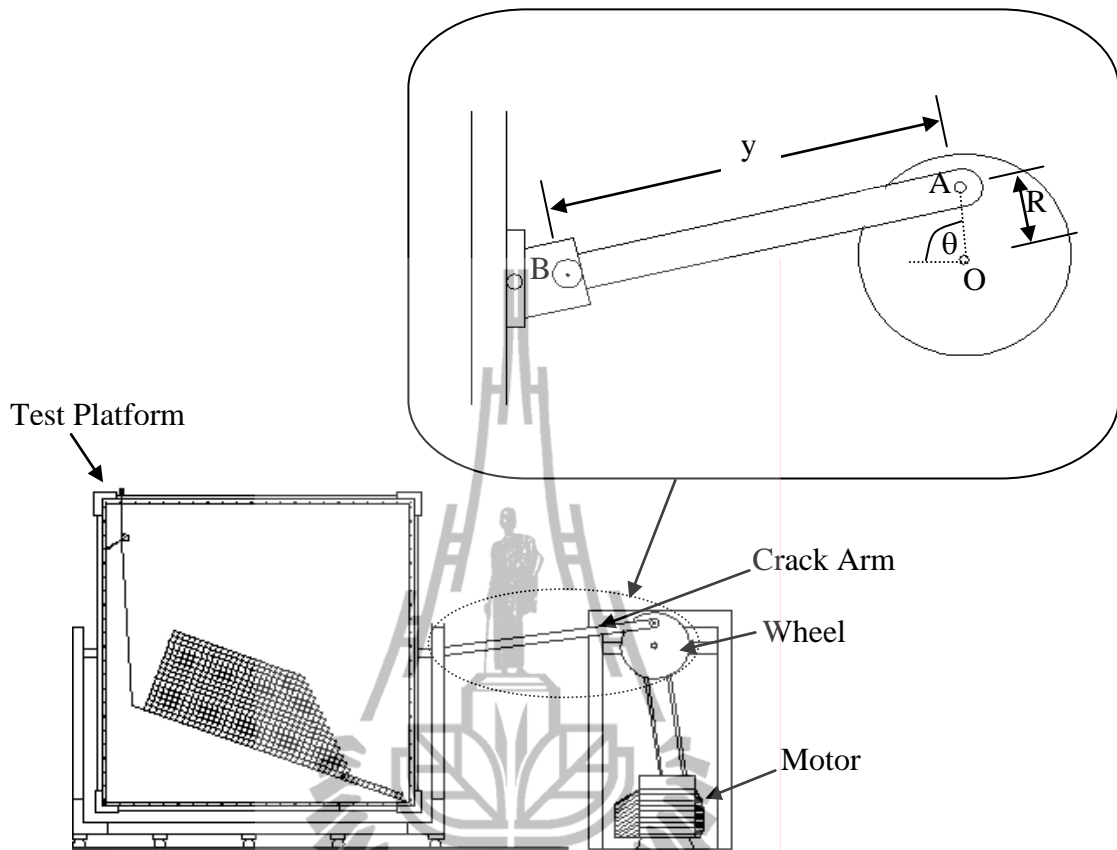


Figure 3.2 Crank arm and flywheel used to induce dynamic loading to the test platform.

where R = radius of wheel, y = length of crack arm, ω_{OA} and ω_{AB} = angular velocity of OA and AB, θ = angle between AO and OB, α_{AB} = relationship between the acceleration of points A and B, and T = duration of flywheel rotation. The angle ϕ can be obtained from:

$$\phi = \sin^{-1} \left[\frac{R \sin \theta}{y} \right] \quad (3.2)$$

The angular velocity of OA and AB can be calculated by:

$$\omega_{OA} = \frac{2\pi}{T}; \quad \omega_{AB} = \frac{R\omega_{OA} \cos \theta}{y \cos \phi} \quad (3.3)$$

The relationship between point A and B, and α_{AB} , is calculated by:

$$\alpha_{AB} = \frac{R\omega_{OA}^2 \sin \theta - y\omega_{AB}^2 \sin \phi}{y \cos \phi} \quad (3.4)$$

The actual rotational duration (T) is monitored for each slope model because different slope geometry and slope mass yield different weights, and hence change the speed of the test platform and the flywheel rotation.

3.3 Rock samples

Phu Phan sandstone from Nakhon Ratchasima province has been selected for use as rock sample here primarily because it has highly uniform texture, density and strength. It is classified as fine-grained quartz sandstone with 72% quartz (0.2-0.8 mm), 20% feldspar (0.1-0.8 mm), 3% mica (0.1-0.3 mm), 3% rock fragments (0.5-2mm), and 2% others (0.5-1 mm). The average density is 2.27 g/cc. (Pangpetch and Fuenkajorn, 2007). The slope models are formed by rectangular and parallelepiped blocks of sandstone with nominal sizes of 4×4×8 cm, 4×4×12 cm, and 4×4×16 cm, as shown in Figures 3.3 and 3.4. They are prepared by saw-cutting and arranged in the frame to simulate rock slopes with two joint sets having strikes parallel to the slope face. The friction angle and cohesion of the saw-cutting surfaces of the Phu Phan sandstone determined by tilt testing are 26 degrees and 0.053 kPa.

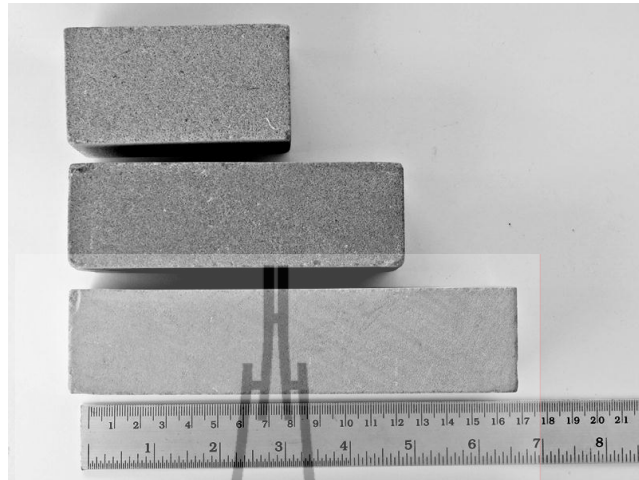


Figure 3.3 Sandstone rectangular blocks with dimensions of 4x4x8 cm, 4x4x12 cm and 4x4x16 cm prepared to simulate joint sets with 90 degrees angle.



Figure 3.4 Parallelogram shaped blocks with dimensions of 4x4x8 cm prepared to simulate joint sets with 135 and 45 degrees intersections.

CHAPTER IV

SLOPE MODEL SIMULATION

4.1 Introduction

This chapter describes the method and results of the slope model simulation. The simulations are made under static and dynamic loading conditions. The simulations are divided into 3 types, including 1) assessment of the joint spacing effects under static condition 2) joint angle effects under static condition, and 3) joint spacing effects under dynamic loading. Over one hundred simulations have been made with the maximum slope height up to 1 m and slope face angles from 35° to 51°. Each set of slope geometries is formed by sandstone blocks with the same dimension, and is simulated at least 3 times to ensure the repeatability of the results. Detailed test procedure is given by Pangpetch and Fuenkajorn (2007). Video records are taken during the test. This allows examining the failure process of the slope models after the test.

4.2 Assessment of the joint spacing effects under static condition

The simulations involve two-dimensional plane sliding of rock slope formed by rectangular blocks of sandstone, under various slope face angles with the slope heights varying from 16 to 100 cm and slope face angles from 40° to 51°. The joint spacing variables are taken as a ratio of the spacing of the horizontal joints to the

spacing of the vertical joints ($S_H: S_V$), as shown in Figure 4.1. This ratios vary from 1:2 (forming by 4×8 cm blocks), 1:3 (forming by 4×12 cm blocks) to 1:4 (forming by 4×16 cm blocks) which each initial slope face angle (ψ_{fo}) of this ratio is 26°, 18° and 14°. The slope height considered here is normalized by the horizontal joint spacing ($H: S_H$) which is varied from 4 to 25. The height of the slope models (H) is calculated by the following equation.

$$H = [h \cdot \sin(\psi_{fo} + \psi_p)] / [\sin(\psi_{fo})] \quad (4.1)$$

where h is the distance between the base and slope top, ψ_{fo} is the initial slope face angle, and ψ_p is the measured sliding plane angle. Table 4.1 summarizes the test parameters and results for effects of joint spacing under static condition. Figure 4.2 through Figure 4.4 shows an example of the failure for a slope model formed by 1:2, 1:3 and 1:4 joint spacing ratios. Figure 4.5 shows simulation results by presenting the slope height at failure as a function of sliding plane angle. Two modes of failures have been observed are plane sliding failure and combination failure (plane and circular failure). For all joint spacing ratios ($S_H: S_V$). The plane sliding failures occurs for low $H: S_H$ ratio. When the $H: S_H$ ratios are high, combination failures are observed. The slope models tend to fail by plane sliding mode when the large joint spacing ratio is used. Plane sliding failures are observed when the slope models are gentle and low, while combination failures are observed when the slopes are steep and high.

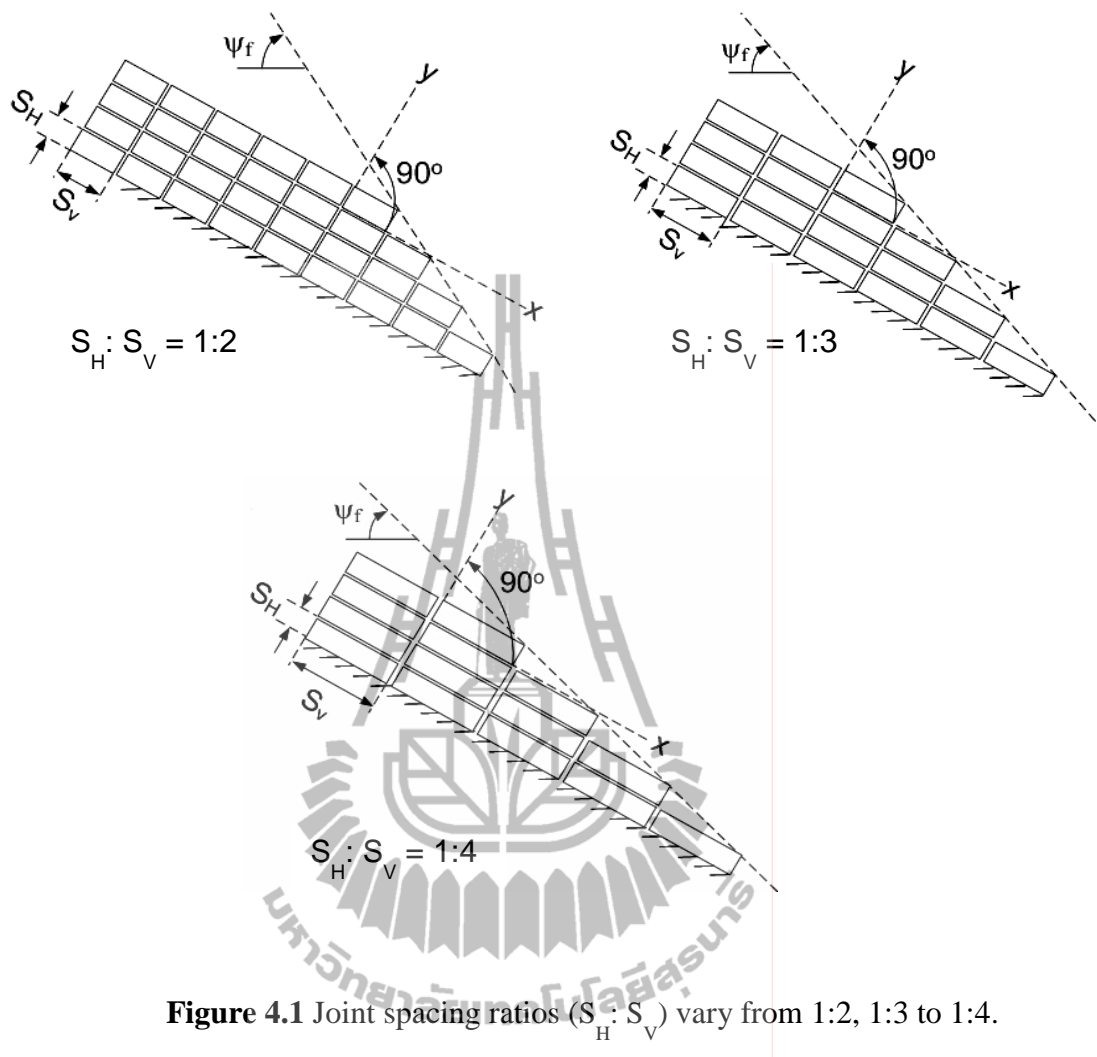
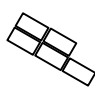
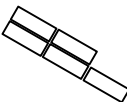
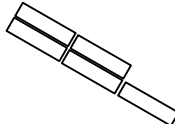


Figure 4.1 Joint spacing ratios ($S_H : S_V$) vary from 1:2, 1:3 to 1:4.

Table 4.1 Summary of simulation parameters and results for joint spacing effects.

$S_H:S_V$	ψ_f	H/S _H	ψ_p	Failure Modes
1:2 	42°-51°	5-9 10-25	23°-25° 16°-22°	Plane Combination
1:3 	40°-45°	4-12 14-20	25°-27° 22°-24°	Plane Combination
1:4 	40°-44°	5-16 17-21	24°-28° 24°-26°	Plane Combination

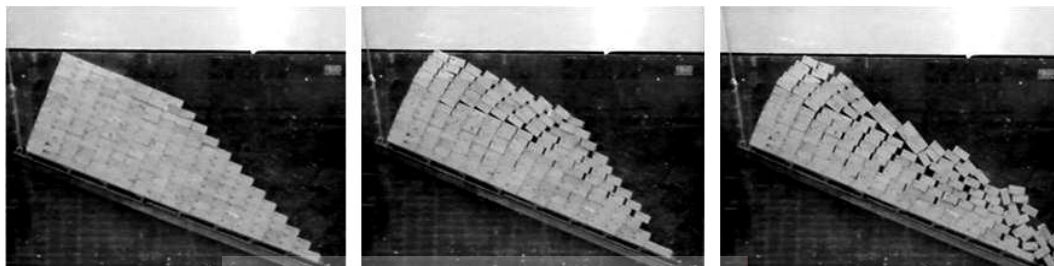


Figure 4.2 Some test results for $S_H:S_V = 1:2$ of combination failure mode.



Figure 4.3 Some test results for $S_H:S_V = 1:3$ of plane failure mode.

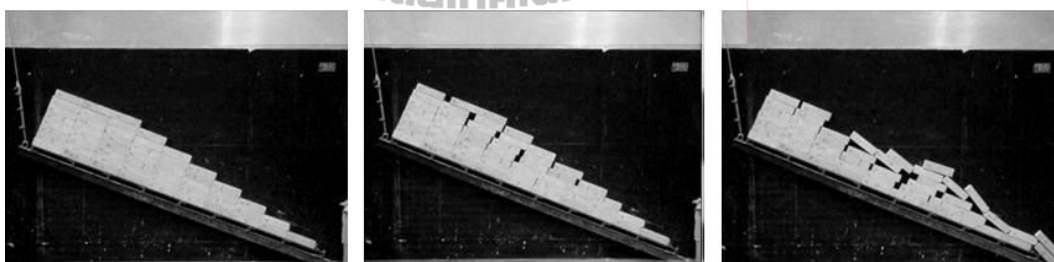


Figure 4.4 Some test results for $S_H:S_V = 1:4$ of plane failure mode.

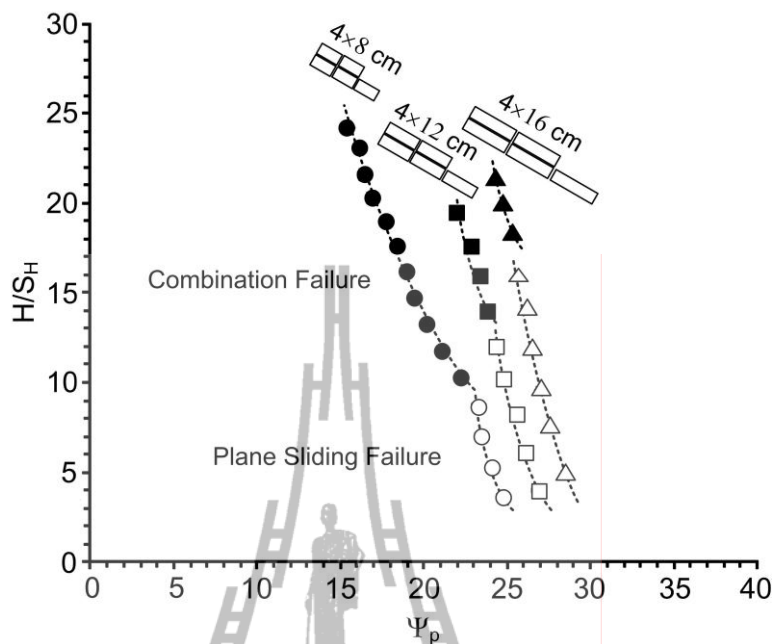


Figure 4.5 Simulation results for $S_H: S_V = 1:2$ (circle symbol), $S_H: S_V = 1:3$ (square symbol) and $S_H: S_V = 1:4$ (triangle symbol) of plane failure mode (white symbol) and combination failure mode (solid symbol).

4.3 Assessment of joint angle effects under static condition

The joint angle simulations of rock slope include three joint angles. The rectangular blocks can simulate the angles between joint sets at 90° . The parallelepiped blocks can simulate the angles between two joint sets at 45° and 135° which initial slope face angles (ψ_{f0}) are between 27° and 14° . The joint spacing ratio is 1:2 (Figure 4.6). The parameters ψ_f and H vary from 35° to 51° and 12 to 100 cm. The height of the slope models (H) is calculated by equation (4.1). Table 4.2 summarizes the test parameters and results to show the effects of joint angle under static condition. Figure 4.7 and Figure 4.8 shows an example of the failure for a slope

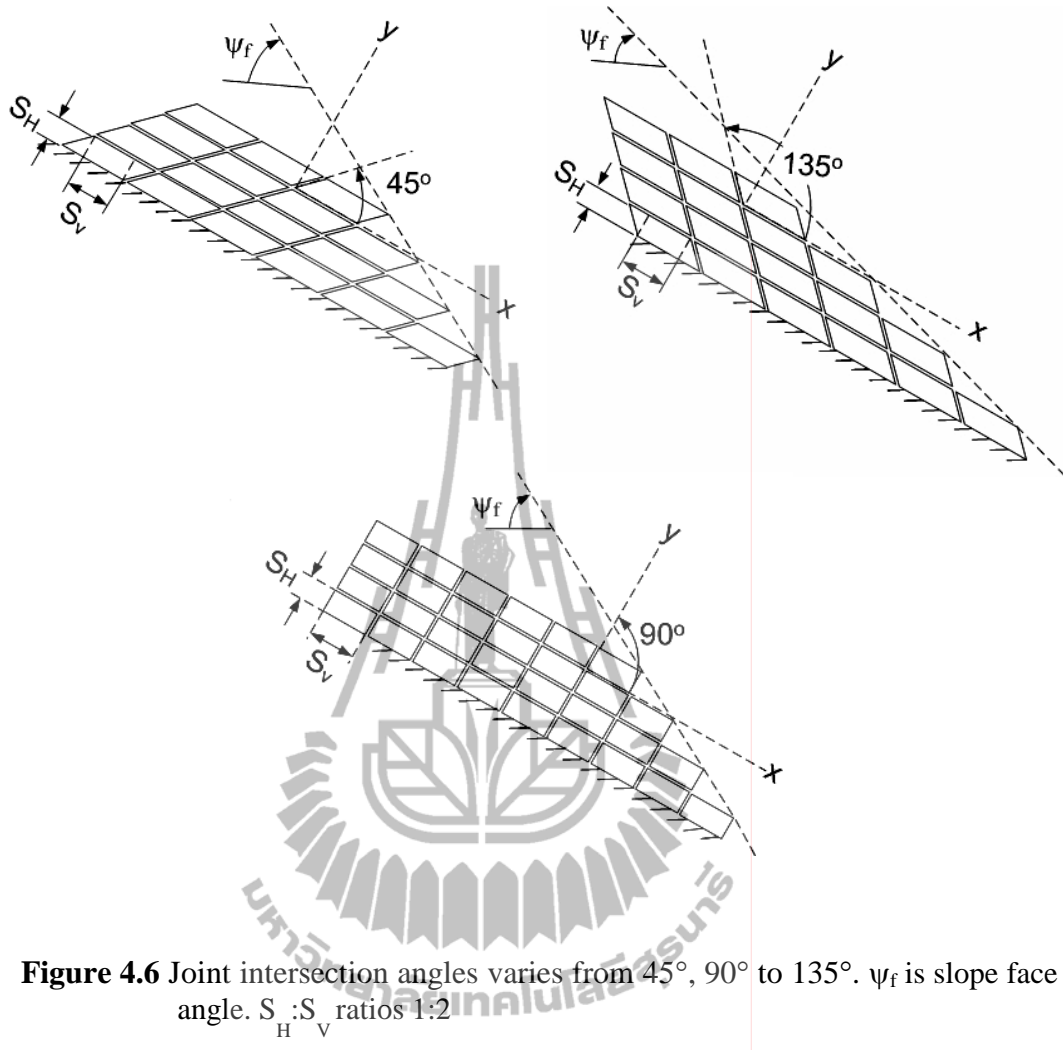
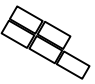
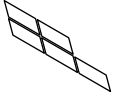
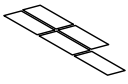


Figure 4.6 Joint intersection angles varies from 45°, 90° to 135°. ψ_f is slope face angle. $S_H : S_V$ ratios 1:2

Table 4.2 Summary of simulation parameters and results for joint angle effect.

Joint set	Ψ_f	H/S _H	Ψ_p	Failure Modes
90° 	42°-51°	5-9 10-25	23°-25° 16°-22°	Plane Combination
135° 	35°-39°	5-18	21°-25°	Plane
45° 	44°-51°	3-17	17°-24°	Plane

**Figure 4.7** Some test results for joint set with 45° intersections of plane failure mode.**Figure 4.8** Some test results for joint set with 135° intersections of plane failure mode.

model of joint set with 45° and 135° intersections. Figure 4.9 shows simulation results by presenting the slope height at failure as a function of sliding plane angle.

The combination failure occurs for joint set with 45° and 135° intersections and for joint set with 90° intersection when the slope models are steep and high gentle and low. The plane sliding failure observed when the slopes are gentle and low. The slopes with joints dipping into the slope face are less stable than those with the joints dipping away from the slope face.

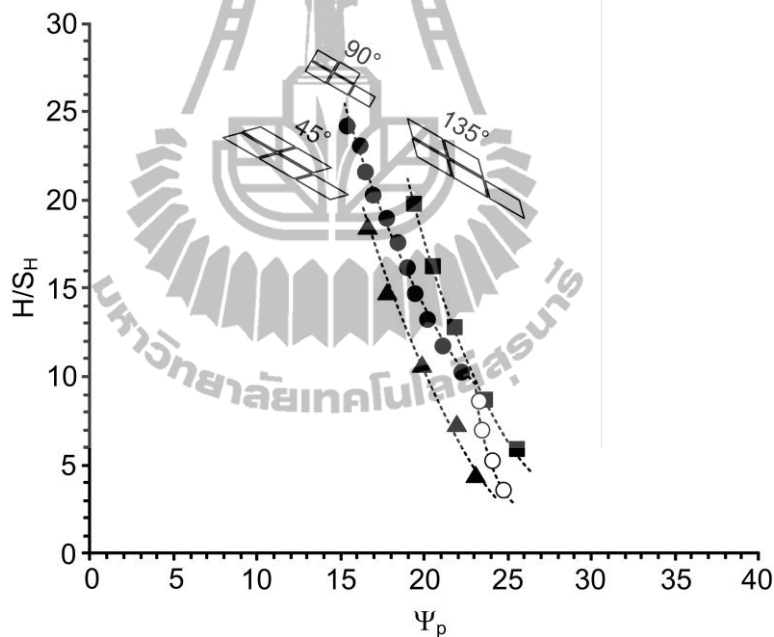
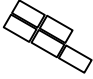
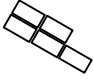
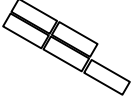
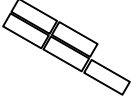
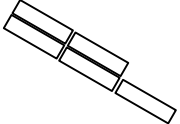
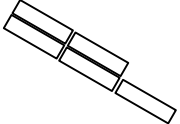
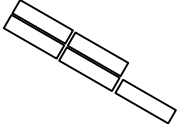


Figure 4.9 Simulation results for joint set with 45° , 90° and 135° intersections of plane failure mode (white symbol) and combination failure mode (solid symbol).

4.4 Assessment of joint spacing effects under dynamic loading

The effect of dynamic loading is studied by considering the effects of the horizontal pseudo-static acceleration induced by cyclic motions of the test platform in the direction parallel to the dip direction of the slope face. These cyclic motions are used to simulate the earthquake shaking. Only the horizontal acceleration is simulated here because it has more impact on the geological structures than does the vertical acceleration (Kramer, 1996). The test procedure is similar to that under static condition. The vertical acceleration is assumed to be zero. The plane sliding failures have been simulated with the horizontal pseudo-static accelerations (a) from 0.09 g to 0.21 g which calculated using equation (3.1). The radius of flywheel (R) and length of crack arm (y) are maintained constant at 2.5 cm and 5.6 cm (Figure 3.2). For all slope geometries the duration for cyclic motion is maintained for one minute. If failure does not occur within one minute of shaking, the sliding plane angle is progressively increased by one degree interval and the test is repeated. The slope models have the sliding plane angles varied from 2° to 13° , slope heights from 21 to 86 cm, and slope face angles from 20° to 38° . Table 4.3 summarizes the test parameters and the results. Figure 4.10 shows the simulation results by presenting the slope height at failure as a function of sliding plane angle for a slope model formed by 1:2, 1:3 and 1:4 joint spacing. Similar to the test results under static condition, the acceleration can reduce the sliding plane angle from 25° to 10° of the under static condition test results, particularly when the $S_H:S_V$ ratio is 1:2. Under similar slope geometry and block arrangement the slope failure induced under dynamic load is less stable than under static loading.

Table 4.3 Summary of simulation parameters and results of rock slope stability analysis under dynamic loading.

$S_H:S_V$	ω_{OA}	ω_{AB}	a (g)	H (cm)	ψ_f	ψ_p	Stability
1:2 	6.1	0.27	0.09	21-86	28°-36°	2°-10°	Stable
					29°-38°	3°-12°	Failure
1:2 	7.3	0.33	0.13	21-28	27°-29°	1°-3°	Stable
					28°-30°	2°-4°	Failure
1:3 	6.1	0.27	0.09	26-82	26°-31°	7°-12°	Stable
					27°-32°	8°-13°	Failure
					7.3	0.33	0.13
1:3 	7.3	0.33	0.13	26-82	23°-29°	4°-10°	Failure
					8.9	0.40	0.21
1:4 	6.1	0.27	0.09	32-84	21°-24°	7°-10°	Stable
					22°-25°	8°-11°	Failure
					7.3	0.33	0.13
1:4 	7.3	0.33	0.13	32-84	21°-24°	7°-10°	Failure
					8.9	0.40	0.21
1:4 	8.9	0.40	0.21	32-84	20°-22°	6°-8°	Failure

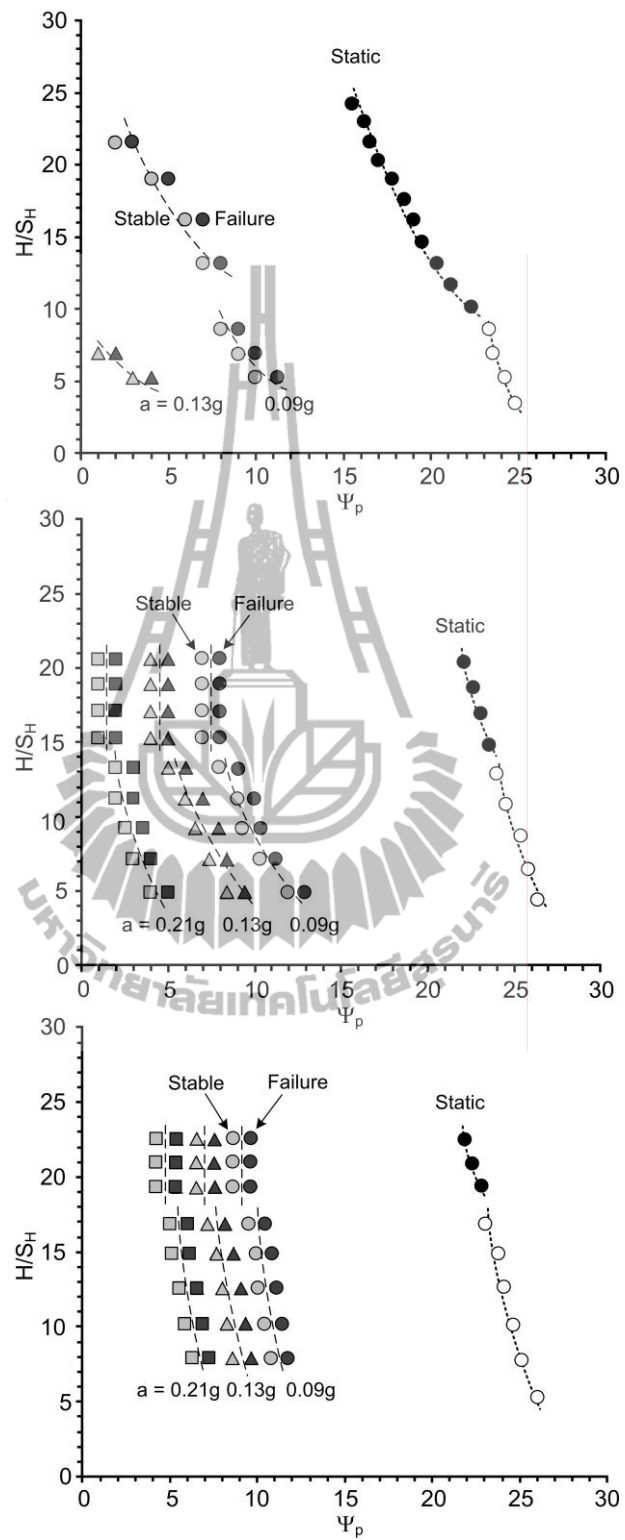


Figure 4.10 Simulation results for $S_H:S_V = 1:2$ (top), $S_H:S_V = 1:3$ (middle) and $S_H:S_V = 1:4$ (bottom) under dynamic loading.

CHAPTER V

DETERMINISTIC METHODS AND NUMERICAL ANALYSIS

5.1 Introduction

This chapter describes the method and results of deterministic methods and the numerical analyses used to calculate the stability of the slope models under static and dynamic loading conditions. The results are compared with those of the model test observations to reveal the predictability of the deterministic methods, the numerical analyses and the performance of the physical modeling.

5.2 Deterministic methods for joint spacing effects under static condition

The simulation results above are compared with the Hoek and Bray's solution for the plane sliding mode and with the simplified Bishop method for the combination mode.

5.2.1 Hoek and Bray's solution

Assuming that the plane sliding mechanism follows the Coulomb criterion, an equation modified from Wyllie and Mah (2004) and Kroeger (2000) is used to calculate the sliding plane angle, as follows;

$$FS = \frac{c \cdot A + (W \cdot \cos \psi_p) \cdot \tan \phi}{W \cdot \sin \psi_p} \quad (5.1)$$

where c is cohesion of rock surface (equal to 0.053 kN/m^2), ϕ is friction angle (equal to 26°), ψ_p is the inclined sliding plane, W is weight of sliding block, and A is the contact area of sliding surface.

$$W = \gamma_r \left[\begin{array}{l} (1 - \cot \psi_f \cdot \tan \psi_p)(bH + \frac{1}{2}H^2 \cdot \cot \psi_f) \\ + \frac{1}{2}b^2(\tan \psi_s - \tan \psi_p) \end{array} \right] \quad (5.2)$$

$$A = (H + b \tan \psi_s - z) \operatorname{cosec} \psi_p \quad (5.3)$$

$$b = H \sqrt{\cot \psi_f \cdot \cot \psi_p - \cot \psi_f} \quad (5.4)$$

$$z = H \left[1 - \cot \psi_f \cdot \tan \psi_p \right] + b \left[\tan \psi_s - \tan \psi_p \right] \quad (5.5)$$

$$H = \frac{z}{1 - \sqrt{\cot \psi_f \tan \psi_p}} \quad (5.6)$$

where ψ_s is the inclined upper slope face, ψ_{f0} is the initial slope face angle, ψ_f is the slope face angle at failure ($\psi_f = \psi_{f0} + \psi_p$), γ_r is the unit weight of rock (equal to $23.8 \times 10^3 \text{ kN/m}^3$ for Phu Phan sandstone), H is height of slope at failure, b is the tension crack location measured from the slope crest, and z is the vertical tension crack depth. The factor of safety of 1.0 is taken to represent the condition at which failure occurs in the slope models.

5.2.2 Simplified Bishop method

Since there is no close-form solution to determine the slope failure under the combination mode, the simplified Bishop method is used to define the lower bound of the critical slope height of the test models. An equation from the simplified Bishop method used here to calculate the factor of safety of a circular failure can be written as follows (Bishop, 1995);

$$FS = [\Sigma X / (1 + Y / FS)] / [\Sigma Z + Q] \quad (5.7)$$

$$X = [c + (\gamma_r \cdot h - \gamma_w \cdot h_w) \cdot \tan \phi] \cdot [\Delta x / \cos \psi_b] \quad (5.8)$$

$$Y = \tan \psi_b \cdot \tan \phi \quad (5.9)$$

$$Z = \gamma_r \cdot h \cdot \Delta x \cdot \sin \psi_b \quad (5.10)$$

$$Q = \frac{1}{2} \gamma_w \cdot Z^2 (\alpha/R) \quad (5.11)$$

where the values of X, Y and Z are calculated for each slice, c is cohesion of rock surface (equal to 0.053 kN/m²), ϕ is friction angle (equal to 26°), ψ_p is the sliding plane angle, ψ_b is base angle, γ_r is unit weight height of each slice, Δx is the width of each slice, assuming that all slices have the same width, The water force Q is added to ΣZ , the sum of the components of the weight of each slice acting parallel to the slide surface. The parameters of simplified Bishop method as show in Figure 5.1. An initial estimate of FS=1 is used.

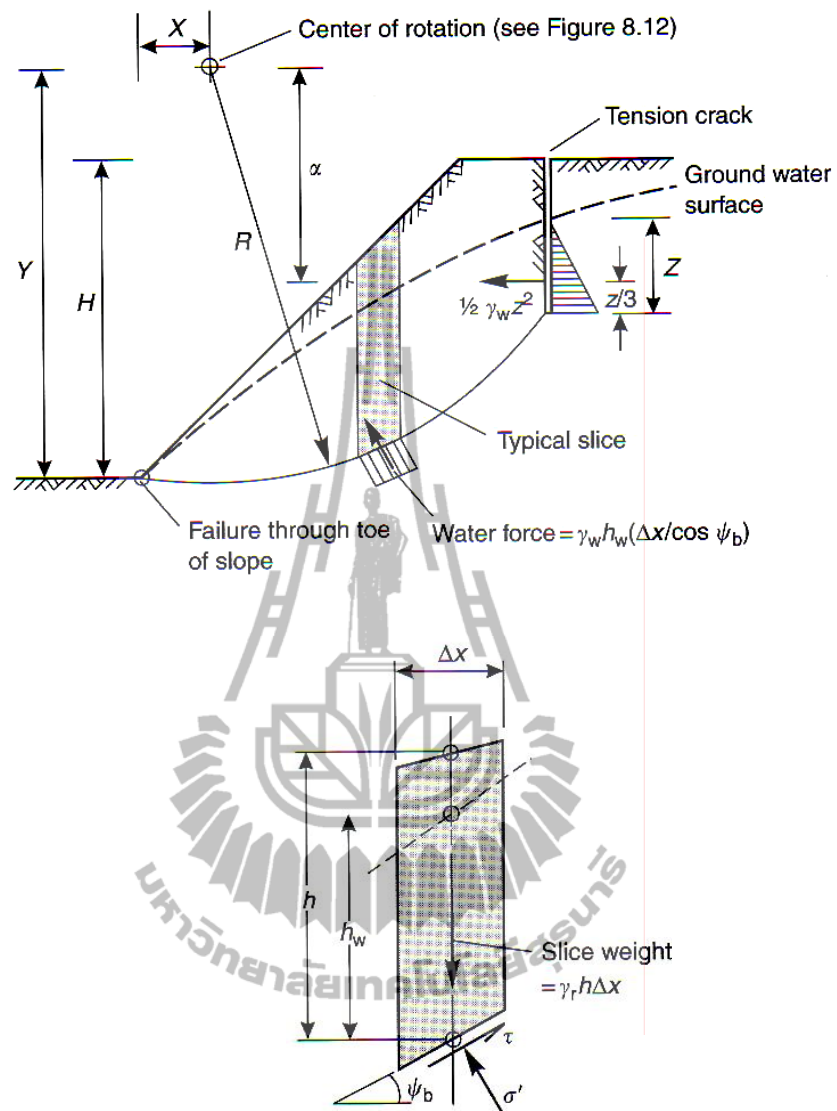


Figure 5.1 Parameters used for calculating the safety factor of a circular failure of simplified Bishop method (Bishop, 1995).

Figure 5.2 compares the calculation results obtained from the two deterministic methods with those of the test models in terms of the slope height ratio as a function of the sliding plane angle. The slope models are more stable as the joint spacing ratio decreases. The transition of the critical slope heights from the pure plane sliding to the combination mode tends to increase as the joint spacing ratio decreases. Under the same sliding angle the Hoek and Bray's prediction gives the critical slope height greater than that of the test models. This suggests that stability analysis using the Hoek and Bray's solution may not be conservative for high slopes formed by jointed rock mass. As expected the simplified Bishop method underestimates the slope height at failure for the combination modes. As the joint spacing ratio increases the differences of the critical slope heights between the Bishop predictions and the test models become smaller.

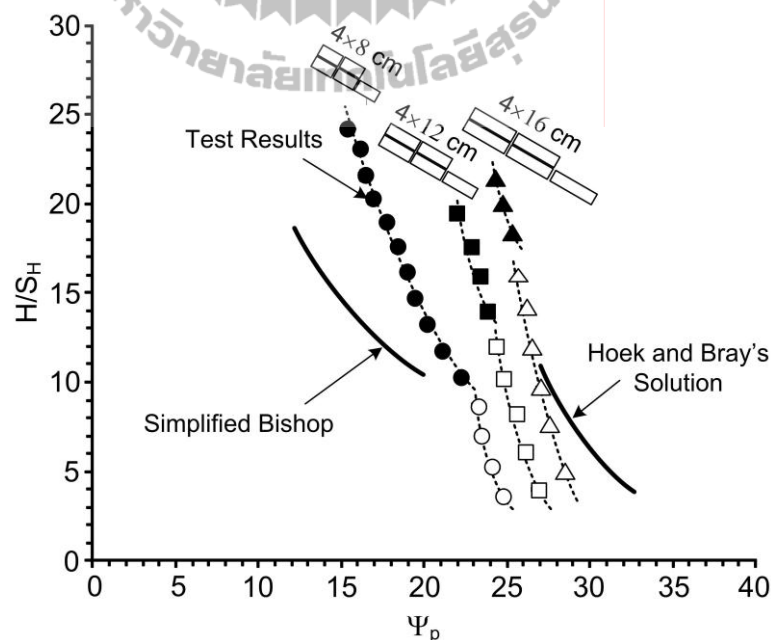


Figure 5.2 Comparisons between test results and deterministic methods for plane sliding mode (white symbol) and combination mode (solid symbol).

5.3 Deterministic methods for joint angle effects under static condition

The test simulation results for the combination mode of failure are compared with the simplified Bishop solution. An equations from the simplified Bishop method are given in equations (5.7) to (5.11). Figure 5.3 compares the critical sliding plane angles observed from the test simulations with those of the simplified Bishop calculation. The combination mode of failure occurs for all slope configurations. The slopes with joints dipping into the slope face are less stable than those with the joints dipping away from the slope face. The simplified Bishop solution underestimates the critical slope height for all cases.

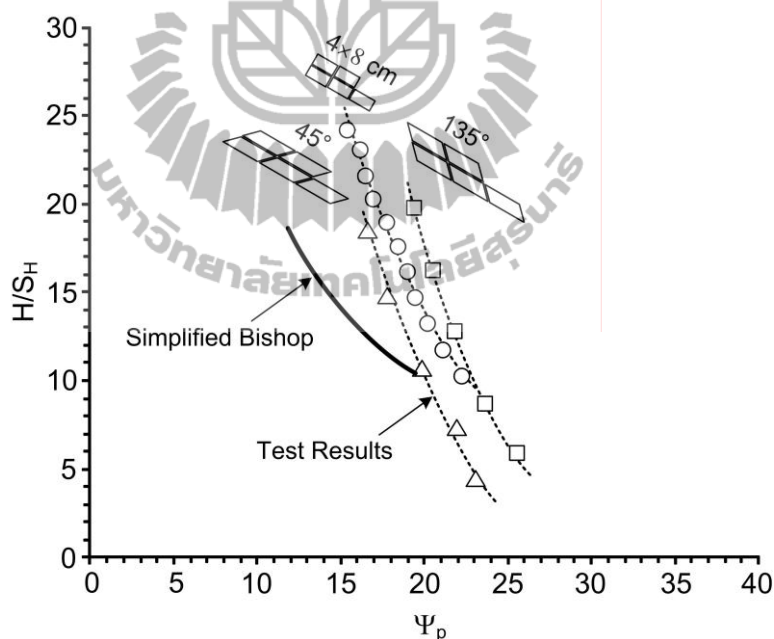


Figure 5.3 Comparisons between test results and simplified Bishop solution for combination mode of failure.

5.4 Deterministic methods for joint spacing effects under dynamic loading

To compare the test results with those calculated by the deterministic method, a closed-form solution given by Kramer (1996) is adopted here. The solution offers a simple approach to calculate the factor of safety of plane failure per unit thickness of slope mass under vertical and horizontal pseudo-static accelerations, as follows.

$$FS = \frac{\text{Resisting force}}{\text{Driving force}} = \frac{c \cdot l + [(W - F_v) \cos \psi_p - F_h \sin \psi_p] \tan \phi}{(W - F_v) \sin \psi_p + F_h \cos \psi_p} \quad (5.12)$$

$$F_h = a W/g = k_h W \quad (5.13)$$

$$F_v = a_v W/g = k_v W \quad (5.14)$$

where F_h and F_v = horizontal and vertical inertial forces, a = horizontal pseudo-static acceleration, a_v = vertical pseudo-static acceleration (assumed here = 0), W = weight of the failure mass, ψ_p = angle of planar failure surface, g = gravitational acceleration, l = the length of the failure plane, and k_h and k_v = dimensionless horizontal and vertical pseudo-static accelerations.

In relation to the earthquake phenomena Kramer (1996) postulates that the horizontal pseudo-static force decreases the factor of safety by reducing the resisting force and increasing the driving force. The vertical pseudo-static force typically has less influence on the factor of safety since it reduces (or increases, depending on its direction) both the driving force and the resisting force. As a result, the effects of

vertical accelerations are frequently neglected in pseudo-static analyses resolving the forces on the potential failure mass in a direction parallel to the failure surface.

In this study the vertical pseudo-static acceleration (a_v) is assumed to be zero, subsequently the vertical inertial force (F_v) becomes zero. This assumption conforms to Kramer's conclusion above. The above equation is therefore reduced to:

$$FS = \frac{c \cdot 1 + [W \cos \psi_p - F_h \sin \psi_p] \tan \phi}{(W \sin \psi_p + F_h \cos \psi_p)} \quad (5.15)$$

By setting $FS=1$, the relationship between the acceleration, a , and the angle of the failure plane, ψ_p , can be developed. Under this condition the acceleration required to induce plane failure for a rock slope decreases with increasing failure plane angle. Figure 5.4 compares the calculation results obtained from the deterministic methods with those of the test models under pseudo-static acceleration (a) are 0.21, 0.13 to 0.09 g in terms of the slope height ratio as a function of the sliding plane angle. The slope models and the Kramer's solution show higher stability as the joint spacing ratio increases. Under the same slope height the Kramer's prediction gives the critical sliding angle greater than that of the test models. This suggests that stability analysis using the Kramer's solution may not be conservative for high slopes formed by jointed rock mass.

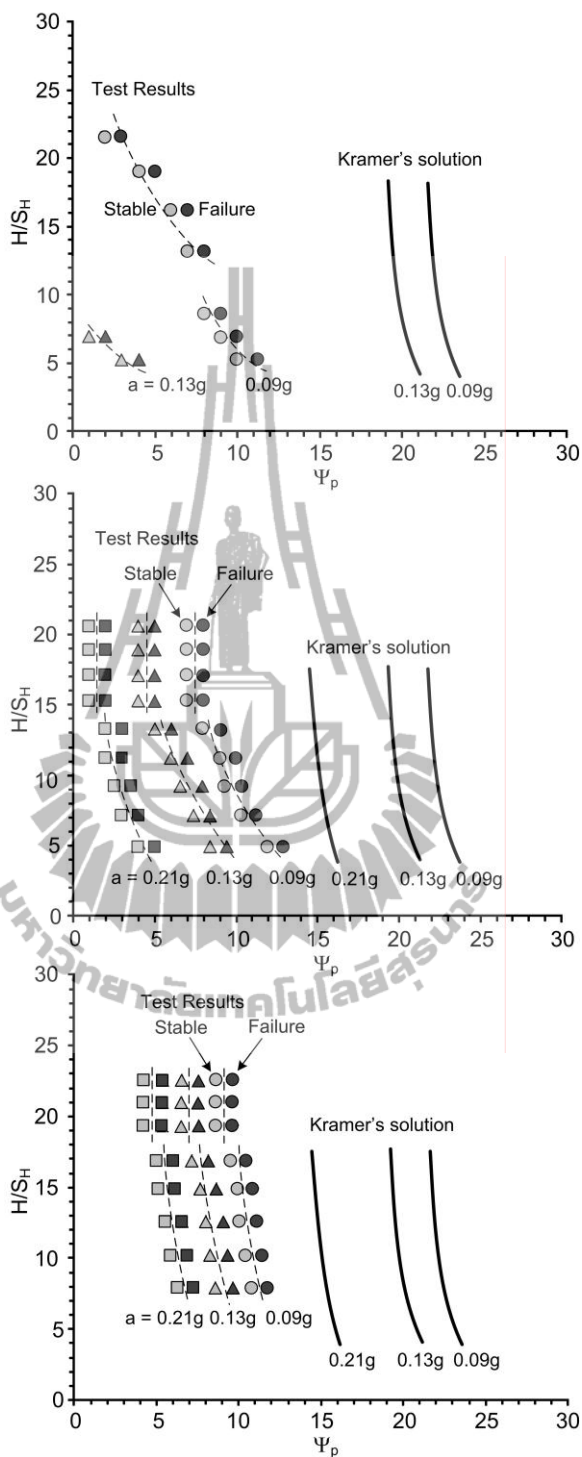


Figure 5.4 Comparisons between test results and deterministic method for various pseudo-static acceleration (a).

5.5 Numerical Analysis of joint spacing effects under static condition

Discrete element analyses are performed using UDEC (Itasca, 2004) to describe the stability conditions of the slope in the physical models. The discrete element models are constructed to represent various slope geometries and joint spacings as used in the physical model testing. The rock block model uses a density of $2,270 \text{ kg/m}^3$ which is equal to the density of Phu Phan sandstone. The bulk modulus and shear modulus of the sandstone are calculated from the elastic modulus and Poisson's ratio as 12.3 GPa and 3.8 GPa. The normal and shear joint stiffness values (K_n and K_s) for the smooth joint in Phu Phan sandstone determined by Suanprom (2009) are 10 GPa/m and 8 GPa/m, respectively. The joint friction angle and cohesion used in the simulations are 26° and 0.053 kPa. They are obtained from the tilt testing. All computer simulations assume plane stress condition. The dilatancy of the joints is assumed to be zero because the surfaces of the tested sandstone blocks are smooth and the cohesion is very low. The corner rounding and the minimum edge length are taken here as 0.001% and 0.002% because the tested sandstone blocks are cubical and rectangular blocks with sharp corners and flat surfaces. Figure 5.5 compares the UDEC results with the test results in form of the slope height ratio (H/S_H) as a function of sliding plane angle (ψ_p). The numerical results agree well with the physical model simulations. Two modes of failure are observed from the UDEC results: pure plane sliding and combination of plane sliding and circular failure. The pure plane sliding mode is obtained from low slope heights with high joint spacing ratios. The combination mode occurs from high slopes with low joint spacing ratios. Under the same sliding plane angle the UDEC results tend to show higher critical slope height for combination failure than do the test models.

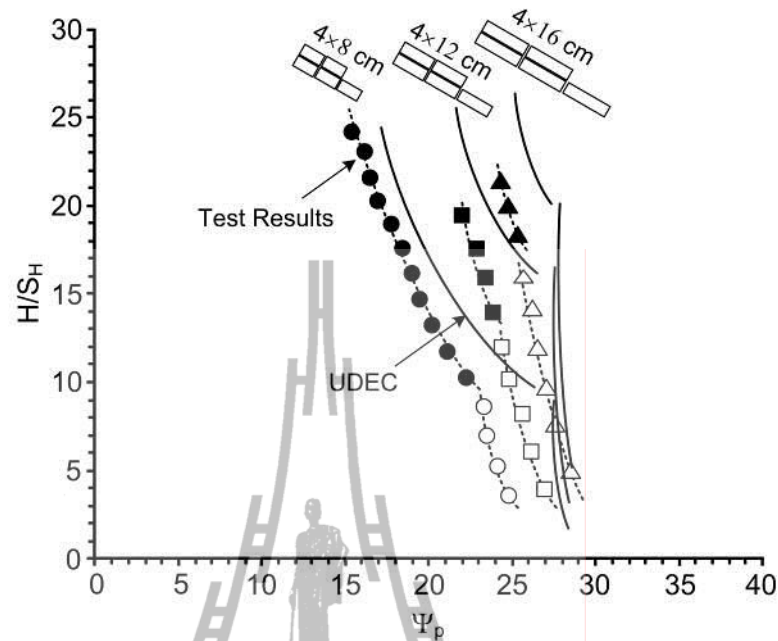


Figure 5.5 Comparisons between test results and UDEC analysis.

Both UDEC and test models indicate that the slopes comprising large joint spacing ratio (e.g., $S_H/S_V = 1:4$) tend to fail by plane sliding while those with smaller joint spacing ratio (e.g., $S_H/S_V = 1:2$) fail under the combination mode. In addition pure plane sliding failure is observed when the slope models are gentle and low, while combination of plane and circular failures is observed when the slopes are steep and high. Figures 5.6 compares the physical model with UDEC results for the 4×8 blocks while the failure is in progress. Similar failure sequence is observed from the two methods of simulation. Failure starts near the slope faces and propagates back into the slope mass.

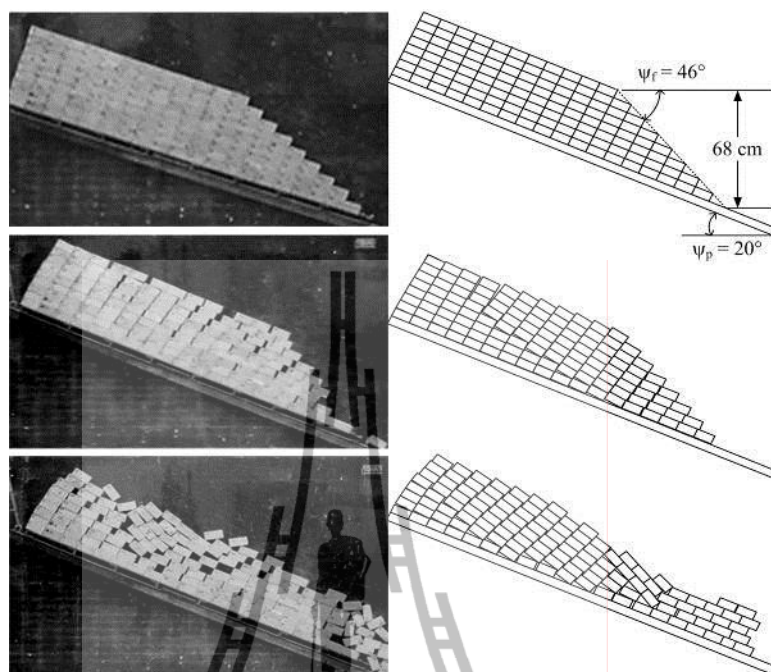


Figure 5.6 Comparisons of test observations (left) with UDEC simulations (right) for 4×8 cm block.

5.6 Numerical Analysis for joint angle effects under static condition

Figure 5.7 compares the UDEC results with the physical model test results in form of the H/S_H ratio as a function of ψ_p . The numerical results agree well with the physical model simulations. Figures 5.8 and 5.9 shows the progressive failure of the physical models and the UDEC predictions for joint sets with 45° and 135° intersections while the failure is in progress. Similar failure sequence is observed from the two methods of simulation. Failure starts near the slope faces and propagates back into the slope mass.

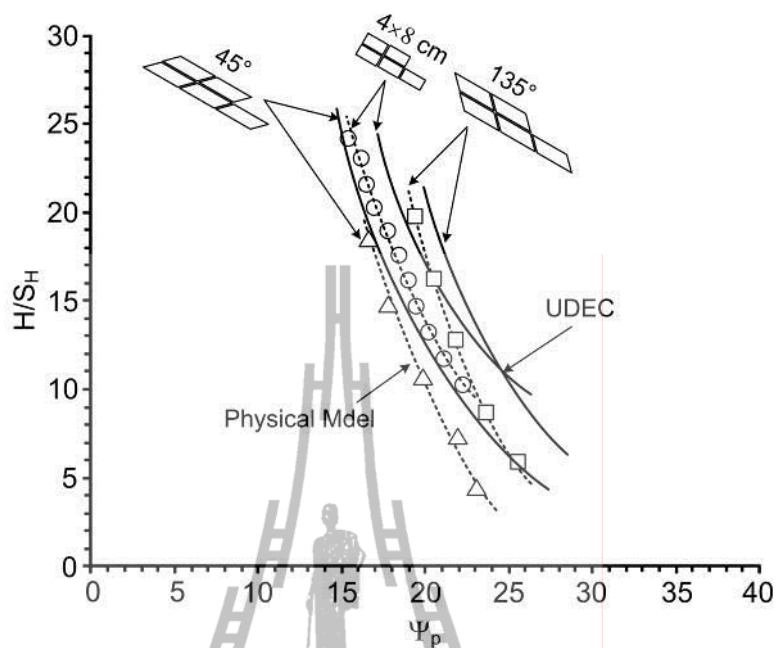


Figure 5.7 Comparisons between test results and UDEC analysis.

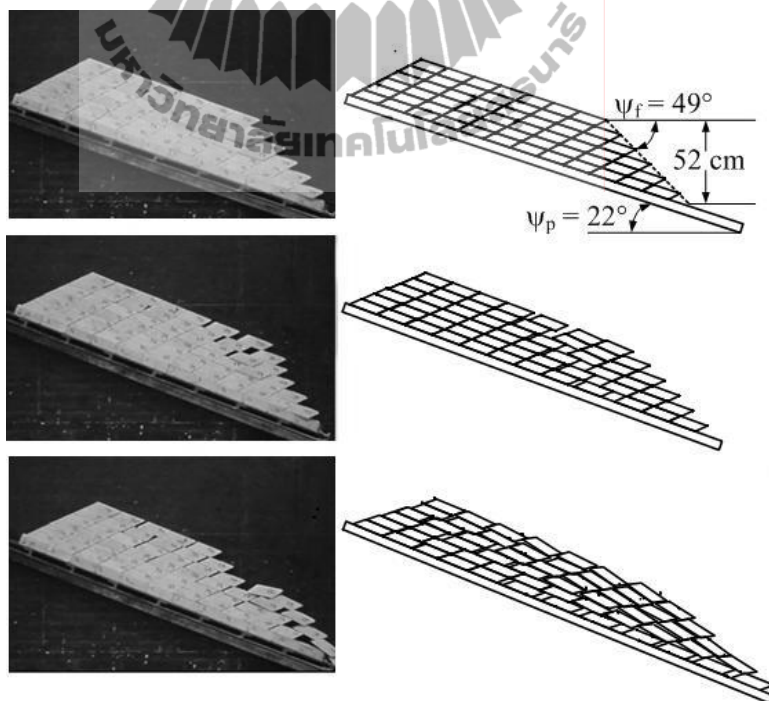


Figure 5.8 Test simulation (left) and UDC result (right) for joint set with 45° intersections.

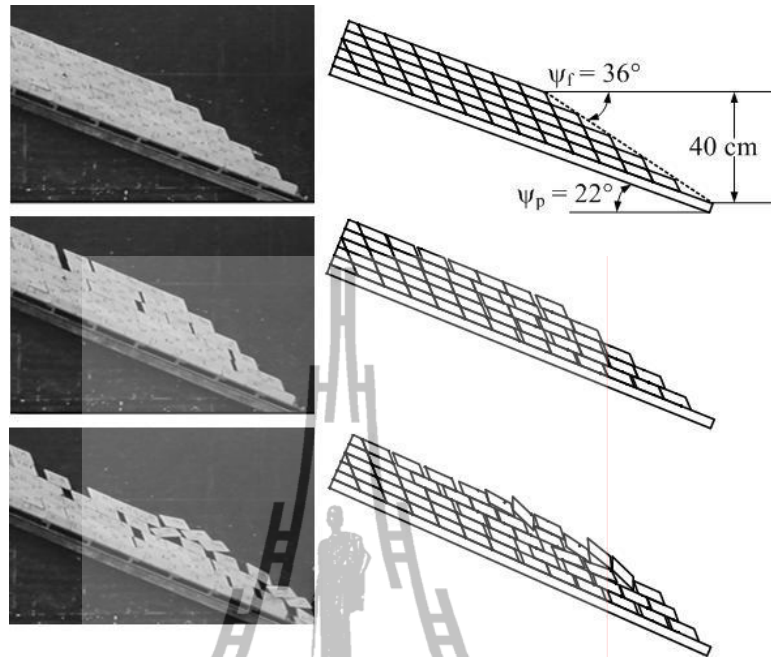


Figure 5.9 Test simulation (left) and UDC result (right) for joint set with 135° intersections.



CHAPTER VI

DISCUSSIONS, CONCLUSIONS, AND RECOMMENDATIONS FOR FUTURE STUDIES

6.1 Discussions

The joints simulated in the slope models here are very smooth and clean with low cohesion and friction angle, which may not truly represent most actual rock joints found under in-situ conditions. The simulation results of joint spacing effects show two modes of failure, plane sliding and combination failure of plane sliding and circular failure. The plane sliding failures occur under low $H:S_H$ ratio. When the $H:S_H$ ratios are high, combination failures are observed. The slope models are more stable as the joint spacing ratio decreases. The transition of the critical slope heights from the pure plane sliding to the combination mode tends to increase as the joint spacing ratio decreases. The simulation results indicate that the deterministic method of Hoek and Bray overestimates the stability conditions of actual slope models under the test parameters used here. As expected the simplified Bishop method underestimates the slope height at failure for the combination modes. As the joint spacing ratio increases the differences of the critical slope heights between the Bishop predictions and the test models become smaller. The numerical results agree well with the physical model simulations. Two modes of failure are also observed from the UDEC results, both UDEC and test models indicate that the slopes

comprising large joint spacing ratio tend to fail by plane sliding while those with smaller joint spacing ratio fail under the combination mode.

The combination failure occurs for joint sets with 45° , 90° , and 135° intersections. The slopes with joints dipping into the slope face are less stable than those dipping away from the slope face. The simplified Bishop solution underestimates the critical slope height for all cases. The numerical results agree well with the physical model simulations. Similar failure sequence is observed from the two methods of simulation. Failure starts near the slope faces and propagates back into the slope mass.

Similar to the test results under static condition, the cyclic loads can reduce the sliding plane angles from 25° to 10° of the under static condition test results, particularly when the $S_H:S_V$ ratio is 1:2. Under similar slope geometry and block arrangement the slope failure induced under cyclic load is less stable than under static loading. The slope models and the Kramer's solution show higher stability as the joint spacing ratio decreases. Under the same slope height the Kramer's prediction gives the critical sliding angle greater than that of the test models.

6.2 Conclusions

A test platform has been constructed for use in the simulation of the scaled-down rock slope models, comprising sets of different joint spacings and joint angles under static condition, and under dynamic loading condition. True gravitational force is used to initiate the failure. The comparisons of the test results with the Hoek and Bray's solution, simplified Bishop's method and UDEC simulations have revealed significant implications that plane sliding dominates when the slopes are gentle and

low with large joint spacing while combination of plane and circular sliding is observed when the slopes are steep and high with small joint spacing. The slope height corresponding to the transition between the two failure modes increases as the joint spacing increases. The maximum height also decreases as the sliding plane angle and slope face angle increase.

The angle between the intersecting joint set and the sliding joint set also affect the maximum slope height. The maximum height at failure is greater when the intersecting joints dip away from the slope face (joint set intersection with 45°) than when they dip toward the slope face (joint set intersection with 135°). These observations agree reasonably well with the results from the UDEC simulations. The simplified Bishop's results underestimate the critical slope height for the combination mode. This is primarily because the solution assumes that the sliding mass is a particulate medium. The results suggested that the deterministic method for the combination failure analysis may be conservative for jointed rock slopes.

The Hoek and Bray's solution severely overestimates the maximum slope height. The discrepancies increase as the joint spacing decreases. This is primarily because the solution assumes that the sliding mass is an intact with block uniform load applying on the sliding surface. This suggests that the Hoek and Bray's solution may not provide a conservative analysis for slopes with open and small joint spacings.

The discrepancy between the deterministic method and the test results under dynamic loading is significant. The deterministic solution proposed by Kramer (1996) overestimates the acceleration which can reduce the sliding plane angle from 25° to 10° , particularly when the $S_H:S_V$ ratio is 1:2. The discrepancy however reduces for slope models formed by larger sandstone blocks and under a greater sliding plane

angle. This is again probably due to the assumption of the continuous mass imposed by the deterministic method. These findings indicate that under dynamic loading plane sliding analysis using the simple deterministic method for rock slopes with joint spacing compared to the slope height will give a nonconservative result.

6.3 Recommendations for future studies

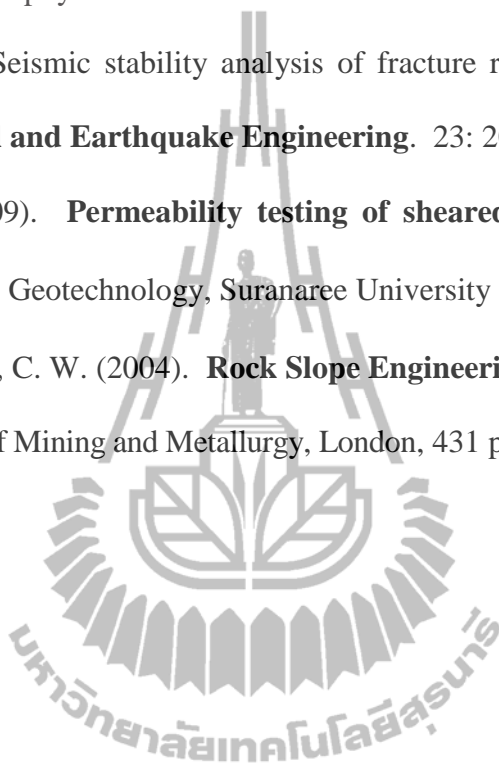
The physical models tested here have a narrow range of the size and shape of the rock blocks used to simulate the joint spacings and joint angles in the test frame. Additional test results obtained from slope models with larger blocks, probably up to 8×8×16 cm to 8×8×32 cm, and with smaller blocks, 2×2×4 cm to 2×2×12 cm, would provide a clearer indication of the effect of joint spacing on slope stability. Additional test results obtained from slope models with joint angle under dynamic loading are desirable. More testing is required to assess the effects of surface roughness, submerging condition and static acceleration. Studying the impact of joint roughness determined from the physical test models is also desirable. It would reveal whether the deterministic methods and the sensitivity of the induced acceleration to the joint roughness are adequate. This may be experimentally assessed by using cast cement blocks with various degrees of pre-defined roughness on the surfaces.

REFERENCES

- Barton, N. R. (1973). Review of a new shear strength criterion for rock joints. **Engineering Geology** 7: 287-332.
- Bishop, A. W. (1995). The use of the slip circle in the stability analysis of earth slope. **Geotechnique** 5: 7-17.
- Goodman, R. E. (1976). **Models of geological engineering in discontinuous rock**. St Paul, Minnesota, USA: West Publishing Company.
- Goodman, R. E. (1989). **Introduction to rock mechanics**. New York: John Wiley & Son.
- Hatzor, Y. H., Arzi, A. A., Zaslavsky, Y., and Shapira, A. (2004). Dynamic stability analysis of jointed rock slopes using the DDA method: King Herod's Palace, Masada, Israel. **International Journal of Rock Mechanics and Mining Sciences** 41(5): 813-832.
- Hoek, E. (1968). Brittle failure of rock. **Rock mechanics in engineering practice**. Edited by K.G. Stagg and O.C. Zienkiewicz. London: J. Willey.
- Hoek, E., and Bray, J.W. (1981). **Rock slope engineering: 3rd edition**. London: Institute of Mining and Metallurgy.
- Itasca (2004). **UDEC 4.0 GUI A Graphical User Interface for UDEC**. Itasca Consulting Group Inc., Minneapolis, MN.
- Kokusho, T., and Ishizawa, T. (2005). Energy approach for earthquake induced slope failure evaluation. **Soil Dynamics and Earthquake Engineering: 1-10**.

- Kramer, S. L. (1996). **Geotechnical earthquake engineering**. New Jersey: Prentice Hall.
- Kroeger, E. B. (2000). The effects of water on planer features in compound slopes. **Environmental & Engineering Geoscience** 6(4): 347-351.
- Latha, M.G., and Garaga, A. (2010). Seismic stability analysis of a Himalayan rock slope. **Rock Mechanics and Rock Engineering** 43:831–843.
- Li, A.J., Lyamin, A.V., and Merifield, R.S. (2009). Seismic rock slope stability charts based on limit analysis methods. **Computers and Geotechnics** 36:135–148.
- Li, S.H., Wang, J.G., Liu, B.S., and Dong, D.P. (2007). Analysis of critical excavation depth for a jointed rock slope using a Face-to-Face discrete element method. **Rock Mechanics and Rock Engineering** 40(4): 331-348.
- Maugeri, M., Musumeci, G., Novita, D., and Taylor, C. A. (2000). Shaking table test of failure of a shallow foundation subjected to an eccentric load. **Soil Dynamics and Earthquake Engineering** 20: 435-444.
- Pangpetch, P., and Fuenkajorn, K. (2007). Simulation of rock slope failure using physical model. In **Proceedings of the First Thailand Symposium on Rock Mechanics** (pp.227-243). Nakhon Ratchasima: Suranaree University of Technology.
- Pangpetch, P., and Fuenkajorn, K. (2009). Physical model simulation of jointed rock slopes under dynamic loads. In **Proceedings of the Second Thailand Symposium on Rock Mechanics** (pp. 131-146). Nakhon Ratchasima: Suranaree University of Technology.
- Patton, F. D. (1966). Multiple modes of shear failure in rock. **Proc. 1 congr. Int. Soc. Rock Mech.** Lisabon. 1: 509-513.

- Riley, W. F. and Sturges, L. D. (1993). **Engineering Mechanics: Dynamics**. John Wiley & Sons, 592 p.
- Roy, S., and Mandal, N. (2009). Modes of hill-slope failure under overburden loads: Insights from physical and numerical models. **Tectonophysics** 473: 324–340.
- Siad, L. (2003). Seismic stability analysis of fracture rock slopes by yield design theory. **Soil and Earthquake Engineering**. 23: 203-212.
- Suanprom, P. (2009). **Permeability testing of sheared fractures in sandstones**. MS. Thesis, Geotechnology, Suranaree University of Technology, 78p.
- Wyllie, D. C., Mah, C. W. (2004). **Rock Slope Engineering: Civil and Mining**. The Institution of Mining and Metallurgy, London, 431 p.





APPENDIX A
PUBLICATIONS

Publications

Kleepmek, M. and Fuenkajorn, K., (2011). **Physical model simulation of jointed rock slopes.** Proceedings of the Third Thailand Symposium on Rock Mechanics, March 10-11, 2011, Cha-Am Beach, Thailand, Published by Geomechanics Research Unit, Suranaree University of Technology, Nakhon Ratchasima, pp. 259-268.

Kleepmek, M., Phueakphum, D., and Fuenkajorn, K., (2011). **Simulation of jointed rock slope using physical model.** In the Proceeding of EIT-Japan Symposium 2011 on Human Security Engineering, Bangkok, Thailand.



Physical model simulation of jointed rock slopes

M. Kleepmek & K. Fuenkajorn

Geomechanics Research Unit, Suranaree University of Technology, Thailand

Keywords: Plane failure, physical model, friction, sandstone

ABSTRACT: Rock slope failures using scaled-down models have been simulated under real gravitational force. The simulation involves two-dimensional plane sliding of rock slopes formed by rectangular blocks of Phu Phan sandstone with nominal sizes of 4×4×8 cm, 4×4×12 cm, and 4×4×16 cm. The sandstone blocks are prepared by saw-cutting arranged to simulate rock slopes with two mutually perpendicular joint sets with different joint spacing ratios of 1:2, 1:3 and 1:4. Pure plane sliding failure is observed when the slope models are gentle and low, while combination of plane and circular failures is observed when the slopes are steep and high. The results agree reasonably well with those obtained from the UDEC simulations. The Hoek and Bray's deterministic method overestimates the critical slope height, particularly for tall slopes with small joint spacing ratios and failed by combination mode. The findings imply that the stability analysis using the deterministic method may not be conservative, particularly for the jointed rock slope with small joint spacings.

1 INTRODUCTION

Physical models or scaled-down models have long been used to simulate the failure behavior of rock slopes in the laboratory. They have been used as teaching and research tools to reveal the two-dimensional failure process of rock slopes under various geological characteristics. They are sometimes employed to gain an understanding of a unique failure process under site-specific conditions. Perhaps the most popular and widely used model is Goodman's friction table (Goodman, 1976). Bray & Goodman (1981) discuss the base friction principle that is used widely to reproduce the effects of gravity in two dimensional physical models of excavations in rock. They develop mathematical principles upon which the analogy between gravity and base friction can be examined. The friction table has later evolved into several versions (e.g. Hittinger, 1978; Teme, 1987; Kim & Lee, 1992; Lanaro et al., 1997). The slope modeling with friction table however poses some disadvantages. The driving force inducing sliding or failure is not a true gravitational force. Instead it largely depends on the friction and velocity of the moving belt, and hence additional calibration or correction is required to reveal the actual slope behavior. A stick-slip behavior between the belt and testing materials is a common problem particularly under low speeds, making the driving force by belt moving unrealistic. Since the friction table is horizontal, or gently inclined, assessment of the true effect of water can not be made.

The objective of this research is to study rock slope failure under static loads by means of laboratory simulation using scaled-down models. The observed results are compared with those calculated by deterministic methods and by numerical analyses (UDEC). A vertical test platform has been used to host the slope models formed by prismatic blocks of Phu Phan sandstone to simulate two-dimensional slope failure. The failure is induced by true gravitational force.

2 TEST PLATFORM

The test platform used in this research is developed by Pangpetch & Fuenkajom (2007), as shown in Figure 1. The frame is hinged through steel rods in the middle to the stand allowing frame rotation from horizontal position during arranging and loading block samples to vertical position for testing under true gravitational force. When the frame is in horizontal position, the aluminum plate becomes a flat bed supporting the rock blocks during loading. The clear and removable acrylic sheet is installed before rotating the frame to the upright position to prevent the block samples from tipping over. It also allows visual inspection and monitoring of slope movement during the test. The test frame can accommodate 4 cm thick rock blocks arranged to a maximum height of up to 1.5 m to simulate two-dimensional jointed rock slopes. Steel grooved rollers mounted underneath the stand are used for testing under dynamic loading. The rollers will be placed on a set of steel rails equipped with a high torque motor, gear system and crank arm to induce a cyclic motion to the entire test platform. The frequency and amplitude of the horizontal pseudo-static acceleration can be controlled by adjusting the rotational diameter of the flywheel and speed of the motor.

3 ROCK SAMPLES

Phu Phan sandstone has been selected for use as rock sample here primarily because it has highly uniform texture, density and strength. It is classified as fine-grained quartz sandstone with 72% quartz (0.2-0.8 mm), 20% feldspar (0.1-0.8 mm), 3% mica (0.1-0.3 mm), 3% rock fragments (0.5-2mm), and 2% others (0.5-1 mm). The average density is 2.27 g/cc. To form slope models with two mutually perpendicular joint sets, rectangular shaped sandstone blocks with nominal sizes of 4×4×8 cm, 4×4×12 cm, and 4×4×16 cm have been prepared by using a saw-cutting machine. The rectangular blocks are used to simulate the joint sets with different spacings. The friction angle and cohesion of the saw-cutting surfaces of the Phu Phan sandstone determined by tilt testing are 21 degrees and 0.053 kPa. The simulated joints have their strike parallel to the slope face, and hence represent a worst case scenario for the stability condition.

4 SLOPE MODELS

Over one hundred slope failure simulations have been carried out under dry condition with the slope heights varying from 16 to 93 cm and slope face angles from 30 to 70 degrees. Each set of slope geometries is formed by sandstone blocks with the same dimension, and is simulated at least 3 times to ensure the repeatability of the results. Detailed test procedure is given by Pangpetch & Fuenkajom (2007). Video records are taken during the test. This allows examining the failure process of the slope models after the test. The joint spacing variables are taken as a ratio of the spacing of the horizontal joints to the spacing of the vertical joints ($S_H : S_V$) as shown in Figure 2. This ratios vary from 1:2 (forming by 4×8 cm blocks), 1:3 (forming by 4×12 cm blocks) to 1:4 (forming by 4×16 cm blocks). The slope height considered here is normalized by the horizontal joint spacing ($H : S_H$) which is varied from 3 to 27.

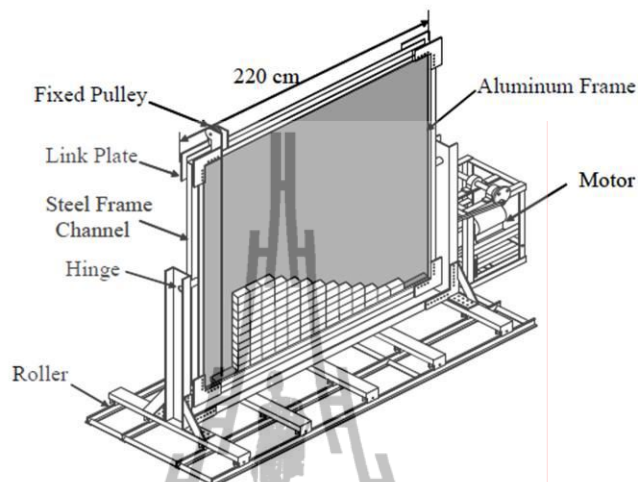


Figure 1. Test frame used in physical model simulation.

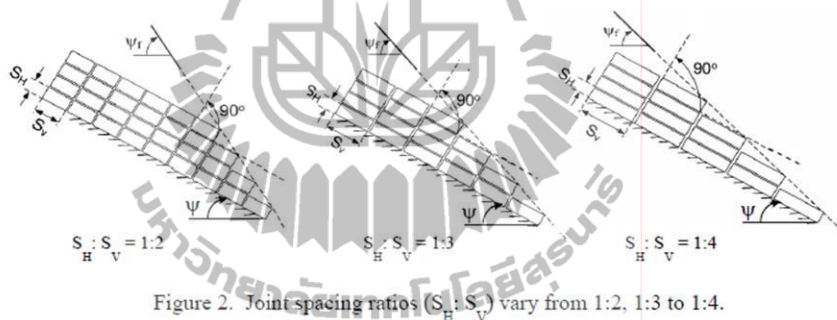


Figure 2. Joint spacing ratios ($S_H : S_V$) vary from 1:2, 1:3 to 1:4.

5 SIMULATION RESULTS

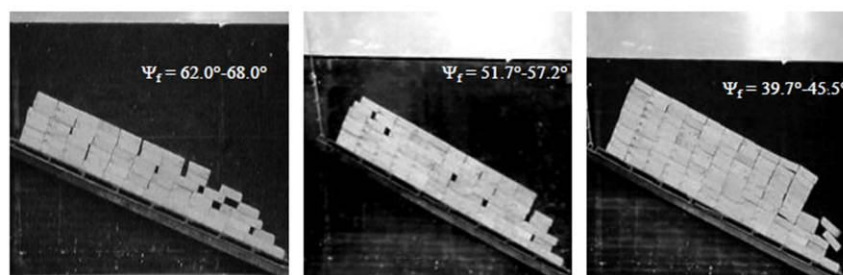
Table 1 summarizes the test parameters and results from the modeling. Figures 3 through 5 show examples of the failure for a slope model formed by 4×8 , 4×12 , and 4×16 cm blocks (i.e., joint spacing ratios, $S_H/S_V = 1:2$, $1:3$ and $1:4$). The height of the slope models (H) is calculated by the following equation.

$$H = \frac{h \cdot \sin(\psi_{f_0} + \psi_p)}{\sin(\psi_{f_0})} \quad (1)$$

where h is the distance between the base and slope top, ψ_{f_0} is the initial slope face angle, and ψ_p is the measured sliding plane angle. Two modes of failure have been observed: pure plane sliding and combination of plane sliding and circular failure. For all joint spacing ratio (S_H/S_V), the pure plane sliding occurs for low $H:S_H$ ratio. When the $H:S_H$ ratios are high,

Table 1. Summary of simulation parameters and results.

$S_H:S_V$	ψ_f (degrees)	H/S_H	ψ_p (degrees)	Failure Modes
1:2	33-39	7.8-12.5 14.5-20.7	23-25 20-22	Plane Plane/Circular
	40-52	3.5-8.6 10.2-24.2	23-25 16-22	Plane Plane/Circular
	58-69	5.2-7.9 10.3-24.4	22-23 15-20	Plane Plane/Circular
1:3	40-46	4.4-18.8	23-27	Plane
	52-57	6.1-18.1 20.8-26.4	22-24 19-20	Plane Plane/Circular
	62-68	5.2-10.6 13.1-23.2	22-23 19-21	Plane Plane/Circular
1:4	32-36	5.3-21.0	23-26	Plane
	44-52	6.9-19.5 21.3-24.7	24-25 22-23	Plane Plane/Circular
	54-57	10.0-13.0 17.0-21.0	22-23 21-22	Plane Plane/Circular

Figure 3. Some test results for various slope heights for $S_H:S_V=1:2$.Figure 4. Some test results for various slope heights for $S_H:S_V=1:3$.

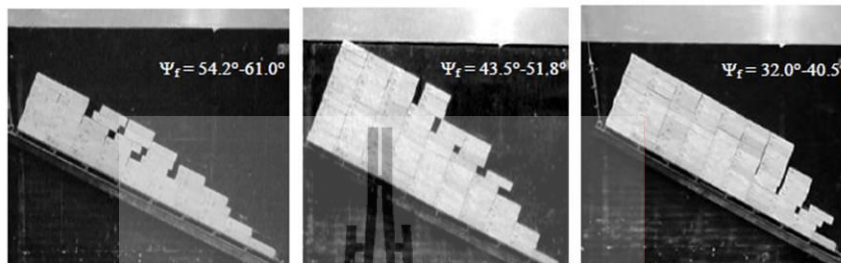


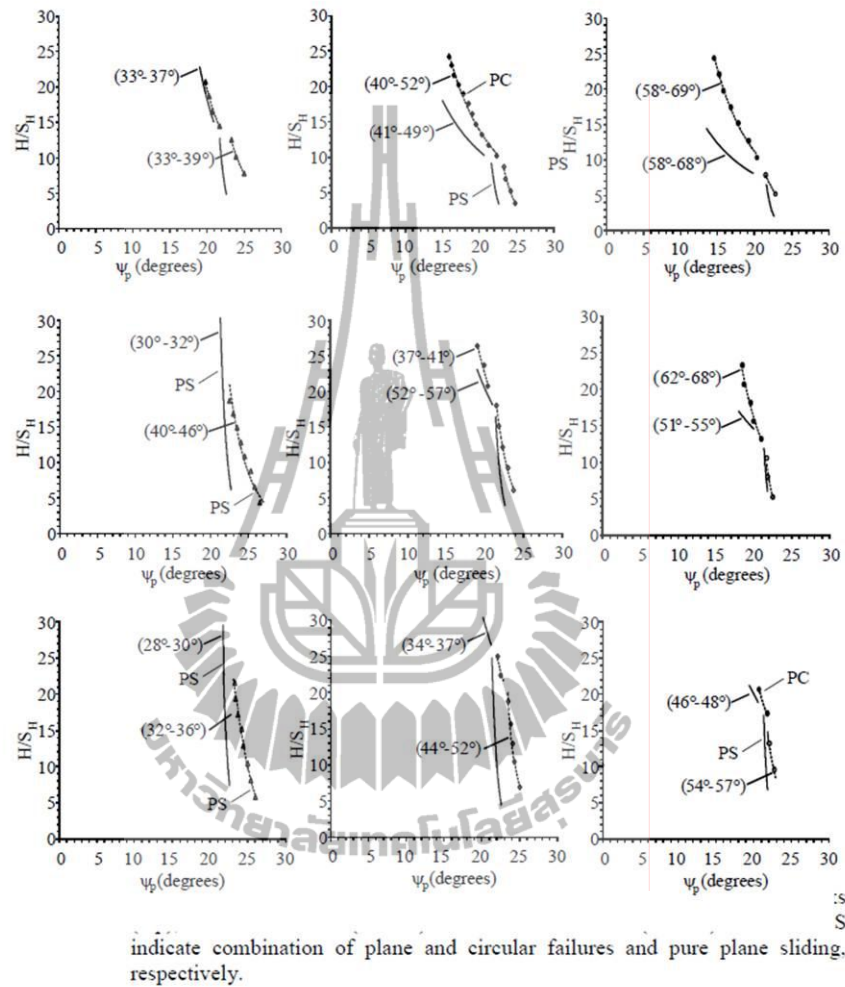
Figure 5. Some test results for various slope heights for $S_H:S_V=1:4$.

combination modes of plane sliding and circular failure are observed. The slope models tend to fail by pure plane sliding mode when the large joint spacing ratio is used. Pure plane sliding failure is observed when the slope models are gentle and low, while combination of plane and circular failures is observed when the slopes are steep and high.

6 DISCRETE ELEMENT ANALYSIS

Discrete element analyses are performed using UDEC (Itasca, 2004) to describe the stability conditions of the slope in the physical models. The discrete element models are constructed to represent various slope geometries and joint spacings as used in the physical model testing. The rock block model uses a density of 2.270 kg m^{-3} which is equal to the density of Phu Phan sandstone. The bulk modulus and shear modulus of the sandstone are calculated from the elastic modulus and Poisson's ratio as 12.3 GPa and 3.8 GPa. The normal and shear joint stiffness values (K_n and K_s) for the smooth joint in Phu Phan sandstone determined by Suanprom (2009) are 10 GPa/m and 8 GPa/m, respectively. The joint friction angle and cohesion used in the simulations are 21° and 0.053 kPa. They are obtained from the tilt testing. All computer simulations assume plane stress condition. The dilatancy of the joints is assumed to be zero because the surfaces of the tested sandstone blocks are smooth and the cohesion is very low. The corner rounding and the minimum edge length are taken here as 0.001% and 0.002% because the tested sandstone blocks are cubical and rectangular blocks with sharp corners and flat surfaces.

Figure 6 compares the UDEC results with the physical model test results in form of the slope height ratio (H/S_H) as a function of sliding plane angle (ψ_b). The numerical results agree well with the physical model simulations. Two models of failure are observed from the UDEC results: pure plane sliding and combination of plane sliding and circular failure. The pure plane sliding mode is obtained from low slope heights with high joint spacing ratios. The combination mode occurs from high slopes with low joint spacing ratio. Under the same sliding plane angle the UDEC results tend to show higher slope height at failure. This is primarily because the rock blocks constructed in the UDEC model are perfectly shaped while small defects exist in the rock blocks used in the physical models. Both UDEC and physical models indicate that the slopes comprising large joint spacing ratio (e.g., $S_H/S_V = 1:4$) tend to fail by plane sliding mode while those with small joint spacing ratio (e.g., $S_H/S_V = 1:2$) fail under pure plane sliding and combination of plane sliding and circular failure. In addition pure plane sliding failure is observed when the slope models are gentle and low, while combination of plane and circular failures is observed when the slopes are steep and high.



Figures 7 and 8 compare the UDEC slope models with the physical slope models while the failure (sliding) is in progress. Similar failure sequence is observed from the two methods of simulation. Failure starts near the slope faces and propagates back into the slope mass.

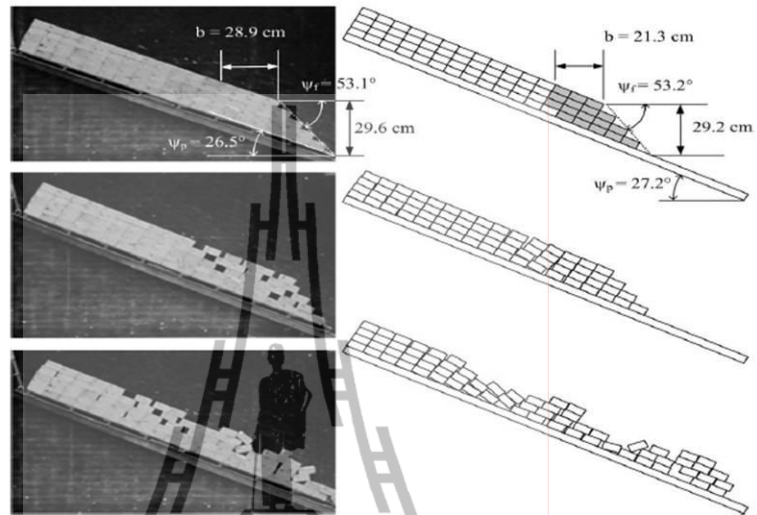


Figure 7. Comparisons of UDEC simulations with physical model tests for 4×8 cm block. The slope height is about 30 cm with slope face of 53 degrees.

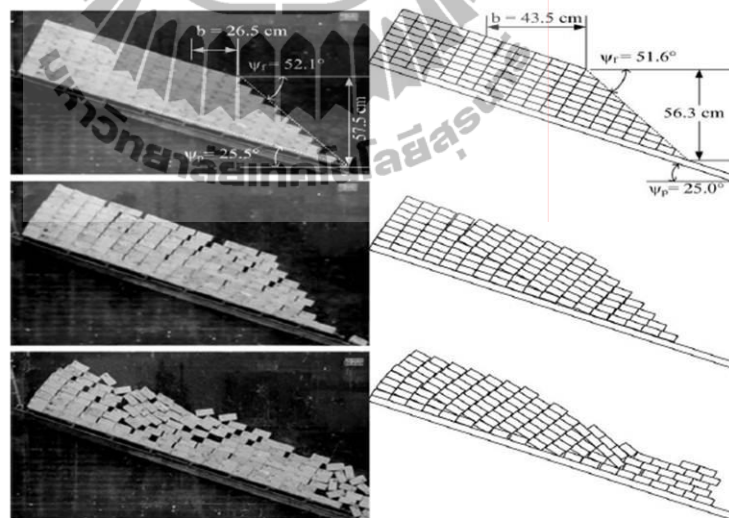


Figure 8. Comparisons of UDEC simulations with physical model tests for 4×8 cm block. The slope height is about 57 cm with slope face of 52 degrees.

7 DETERMINISTIC METHOD

Assuming that the plane sliding mechanism follows the Coulomb criterion, the deterministic method uses an equation modified from [Wyllie et al. \(2004\)](#) and [Kroeger \(2000\)](#) to calculate the sliding plane angle as show below:

$$FS = \frac{c \cdot A + (W \cdot \cos \psi_p) \cdot \tan \phi}{W \cdot \sin \psi_p} \quad (2)$$

where c is cohesion of rock surface (equal to 0.053 kN/m^2), ϕ is friction angle (equal to 21 degrees), ψ_p is the inclined sliding plane, W is weight of sliding block, and A is the contact area of sliding surface.

$$W = \gamma_r \left[(1 - \cot \psi_f \cdot \tan \psi_p) \left(bH + \frac{1}{2} H^2 \cdot \cot \psi_f \right) + \frac{1}{2} b^2 (\tan \psi_s - \tan \psi_p) \right] \quad (3)$$

$$A = (H + b \tan \psi_s - z) \operatorname{cosec} \psi_p \quad (4)$$

$$b = H \sqrt{\cot \psi_f \cdot \cot \psi_p - \cot \psi_f} \quad (5)$$

$$z = H \left[1 - \cot \psi_f \cdot \tan \psi_p \right] + b \left[\tan \psi_s - \tan \psi_p \right] \quad (6)$$

where ψ_s is the inclined upper slope face, ψ_{i0} is the initial slope face angle, ψ_f is the slope face angle at failure ($\psi_f = \psi_{i0} + \psi_p$), γ_r is the unit weight of rock (equal to $23.8 \times 10^3 \text{ kN/m}^3$ for Phu Phan sandstone), H is height of slope at failure, b is the tension crack location measured from the slope crest, and z is the vertical tension crack depth. The factor of safety of 1.0 is taken to represent the condition at which failure occurs in the slope models.

Figure 9 compares the sliding angles obtained from the deterministic method with those of the physical model tests for the same slope geometry. Under the same sliding angle the deterministic method overestimates the slope height at failure for the slopes fail by combination modes. It however slightly underestimates the slope height at failure for those fail by pure plane sliding. This behavior is clearly pronounced for the slopes with small joint spacing ratios. The results suggest that stability analysis using the deterministic method may not be conservative for jointed rock slopes.

8 DISCUSSIONS AND CONCLUSIONS

It is recognized that the joints simulated in the slope models here are very smooth and clean with low cohesion and friction angle, which may not truly represent most actual rock joints found in in-situ rock slopes. Nevertheless the comparisons of the test results with the deterministic solutions (by [Hoek & Bray, 1981](#)) and computer simulations (UDEC code) under the same test parameters (e.g., joint properties and slope characteristics) have revealed significant implications. The deterministic method and computer simulation over-estimate the sliding plane angles, particularly for the slope models with small joint spacings. This is

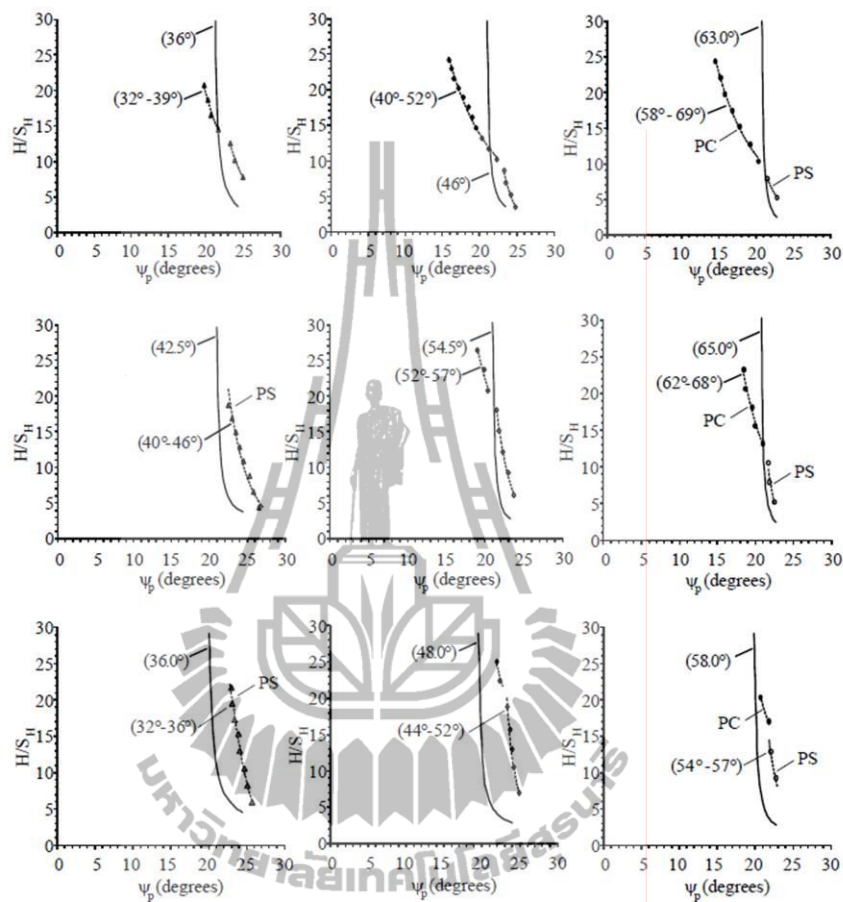


Figure 9. Comparisons between test results and deterministic method for 4×8 cm blocks, 4×12 cm blocks and 4×16 cm blocks. PC and PS indicate combination of plane and circular failures and pure plane sliding, respectively.

probably due to the impacts of the block spacing, block shape and interaction forces between the discrete blocks in the sliding mass. This implies that stability analysis by assuming that the sliding mass is continuous as used by the deterministic method may not be conservative, particularly for slope masses with short-spaced joints compared to the slope height. cast cement blocks with various degrees of pre-defined roughness on the surfaces.

ACKNOWLEDGEMENT

This research is funded by Suranaree University of Technology. Permission to publish this paper is gratefully acknowledged.

REFERENCES

- Bray, J.W. & Goodman, R.E., 1981. The theory of base friction models. *International Journal of Rock Mechanics and Mining Science and Geomechanics*, 18(6): 453-468.
- Goodman, R.E., 1976. *Models of geological engineering in discontinuous rock*. West Publishing Company, St Paul, Minnesota, USA.
- Hittinger, M., 1978. *Numerical analysis of toppling failures in jointed rock*, Ph.D. Thesis, University of California, Berkeley, USA.
- Hoek, E. & Bray, J.W., 1981. *Rock slope engineering*, 3rd edition, Institute of Mining and Metallurgy, London.
- Itasca, 2004. *UDEC 4.0 GUIA Graphical User Interface for UDEC*. Itasca Consulting Group Inc., Minneapolis, MN.
- Kim, Y.G. & Lee, H.K., 1992. Slope stability analysis in discontinuous rocks by base friction model test and its numerical analysis. *Regional Symposium on Rock Slopes*. Coal India Limited, India. pp. 195-201.
- Kroeger, E.B. 2000. Analysis of plane failures in compound slopes. *International Journal of Surface Mining, Reclamation and Environment* 14: 215-222.
- Lanaro, F., Jing, L., Stephansson, O. & Barla, G., 1997. D.E.M. Modeling of laboratory tests of block toppling. *International Journal of Rock Mechanics and Mining Sciences*, 34(3-4): 173.
- Pangpetch, P. & Fuenkajorn, K., 2007. Simulation of rock slope failure using physical model. In *Proceedings of the First Thailand Symposium on Rock Mechanics*. Suranaree University of Technology, Nakhon Ratchasima. pp. 227-243.
- Suanprom, 2009. Permeability testing of sheared fractures in sandstones. MS. Thesis, Geotechnology, Suranaree University of Technology. 78 pp.
- Teme, S.C., 1987. A kinematic modeling machine for rock slope studies. *International Journal of Mining and Geological Engineering*, 5: 75-81.
- Terzaghi, K., 1950. Mechanisms of landslides. In *Application of Geology to Engineering Practice*. Geol. Soc. of America, New York, Berkey, pp. 83-123.
- Wyllie, D.C., Mah, C.W. & Hoek, E. 2004. *Rock Slope Engineering: Civil and Mining*. The Institution of Mining and Metallurgy, London.

Simulation of Jointed Rock Slopes using Physical Model

Matsee Kleepmek*, Decho Phueakphum and Kittitip Fuenkajorn

Geomechanics Research Unit, Institute of Engineering,
Suranaree University of Technology,
Muang District, Nakhon Ratchasima, Thailand 30000.
Phone (66-44) 223-363, Fax (66-44) 224-448
E-Mail: matseekleepmek@gmail.com

ABSTRACT: Rock slope failures using scaled-down models have been simulated under real gravitational force. The simulation involves two-dimensional plane sliding of rock slopes formed by rectangular blocks of Phu Phan sandstone with nominal sizes of 4×4×8 cm, 4×4×12 cm, and 4×4×16 cm. The sandstone blocks are prepared by saw-cutting arranged to simulate rock slopes with two mutually perpendicular joint sets with different joint spacing ratios of 1:2, 1:3 and 1:4. Pure plane sliding failure is observed when the slope models are gentle and low, while combination of plane and circular failures is observed when the slopes are steep and high. The results agree reasonably well with those obtained from the UDEC simulations. The Hoek and Bray's deterministic method overestimates the critical slope height, particularly for tall slopes with small joint spacing ratios and failed by combination mode. The findings imply that the stability analysis using the deterministic method may not be conservative, particularly for the jointed rock slope with small joint spacings.

Keywords: Plane failure, physical model, friction, sandstone

1. INTRODUCTION

Physical models or scaled-down models have long been used to simulate the failure behavior of rock slopes in the laboratory. They have been used as teaching and research tools to reveal the two-dimensional failure process of rock slopes under various geological characteristics. They are sometimes employed to gain an understanding of a unique failure process under site-specific conditions. Perhaps the most popular and widely used model is Goodman's friction table (Goodman, 1976). Bray & Goodman (1981) discuss the base friction principle that is used widely to reproduce the effects of gravity in two dimensional physical models of excavations in rock. They develop mathematical principles upon which the analogy between gravity and base friction can be examined. The friction

table has later evolved into several versions (e.g. Hittinger, 1978; Teme, 1987; Kim & Lee, 1992; Lanaro et al., 1997). The slope modeling with friction table however poses some disadvantages. The driving force inducing sliding or failure is not a true gravitational force. Instead it largely depends on the friction and velocity of the moving belt, and hence additional calibration or correction is required to reveal the actual slope behavior. A stick-slip behavior between the belt and testing materials is a common problem particularly under low speeds, making the driving force by belt moving unrealistic. Since the friction table is horizontal, or gently inclined, assessment of the true effect of water can not be made.

The objective of this research is to study rock slope failure under static loads by means of laboratory simulation using scaled-down models. The observed results are compared

with those calculated by deterministic methods and by numerical analyses (UDEC). A vertical test platform has been used to host the slope models formed by prismatic blocks of Phu Phan sandstone to simulate two-dimensional slope failure. The failure is induced by true gravitational force.

2. TEST PLATFORM

The test platform used in this research is developed by Pangpetch & Fuenkajorn (2007), as shown in Figure 1. The frame is hinged through steel rods in the middle to the stand allowing frame rotation from horizontal position during arranging and loading block samples to vertical position for testing under true gravitational force. When the frame is in horizontal position, the aluminum plate becomes a flat bed supporting the rock blocks during loading. The clear and removable acrylic sheet is installed before rotating the frame to the upright position to prevent the block samples from tipping over. It also allows visual inspection and monitoring of slope movement during the test. The test frame can accommodate 4 cm thick rock blocks arranged to a maximum height of up to 1.5 m to simulate two-dimensional jointed rock slopes. Steel grooved rollers mounted underneath the stand are used for testing under dynamic loading. The rollers will be placed on a set of steel rails equipped with a high torque motor, gear system and crank arm to induce a cyclic motion to the entire test platform. The frequency and amplitude of the horizontal pseudo-static acceleration can be controlled by adjusting the rotational diameter of the flywheel and speed of the motor.

3. ROCK SAMPLES

Phu Phan sandstone has been selected for use as rock sample here primarily because it has highly uniform texture, density and strength. It is classified as fine-grained quartz sandstone with 72% quartz (0.2-0.8 mm), 20% feldspar (0.1-0.8 mm), 3% mica (0.1-0.3 mm), 3% rock fragments (0.5-2mm), and 2% others (0.5-1 mm). The average density is 2.27 g/cc. To form slope models with two mutually perpendicular joint sets, rectangular shaped

sandstone blocks with nominal sizes of 4×4×8 cm, 4×4×12 cm, and 4×4×16 cm have been prepared by using a saw-cutting machine. The rectangular blocks are used to simulate the joint sets with different spacings. The friction angle and cohesion of the saw-cutting surfaces of the Phu Phan sandstone determined by tilt testing are 21 degrees and 0.053 kPa. The simulated joints have their strike parallel to the slope face, and hence represent a worst case scenario for the stability condition.

4. SLOPE MODELS

Over one hundred slope failure simulations have been carried out under dry condition with the slope heights varying from 16 to 93 cm and slope face angles from 30 to 70 degrees. Each set of slope geometries is formed by sandstone blocks with the same dimension, and is simulated at least 3 times to ensure the repeatability of the results. Detailed test procedure is given by Pangpetch & Fuenkajorn (2007). Video records are taken during the test. This allows examining the failure process of the slope models after the test. The joint spacing variables are taken as a ratio of the spacing of the horizontal joints to the spacing of the vertical joints ($S_H : S_V$) as shown in Figure 2. This ratios vary from 1:2 (forming by 4×8 cm blocks), 1:3 (forming by 4×12 cm blocks) to 1:4 (forming by 4×16 cm blocks). The slope height considered here is normalized by the horizontal joint spacing ($H : S_H$) which is varied from 3 to 27.

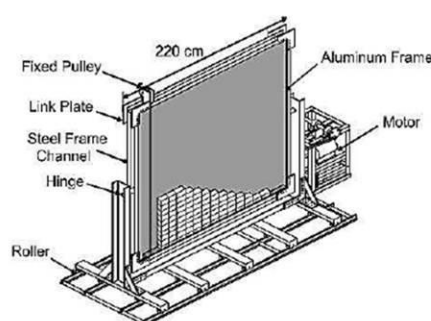


Figure 1. Test frame used in physical model simulation.

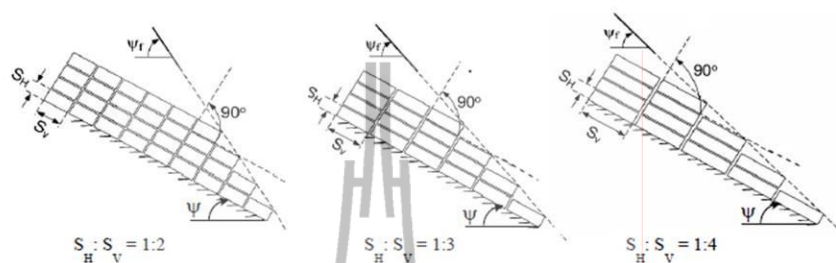


Figure 2. Joint spacing ratios ($S_H : S_V$) vary from 1:2, 1:3 to 1:4.

5. SIMULATION RESULTS

Table 1 summarizes the test parameters and results from the modeling. Figures 3 through 5 show examples of the failure for a slope model formed by 4×8 , 4×12 , and 4×16 cm blocks (i.e., joint spacing ratios, $S_H/S_V = 1:2$, $1:3$ and $1:4$). The height of the slope models (H) is calculated by the following equation.

$$H = \frac{h \cdot \sin(\psi_{fo} + \psi_p)}{\sin(\psi_{fo})} \quad (1)$$

where h is the distance between the base and slope top, ψ_{fo} is the initial slope face angle, and ψ_p is the measured sliding plane angle. Two modes of failure have been observed: pure plane sliding and combination of plane sliding and circular failure. For all joint spacing ratio (S_H/S_V), the pure plane sliding occurs for low H/S_H ratio. When the H/S_H ratios are high, combination modes of plane sliding and circular failure are observed. The slope models tend to fail by pure plane sliding mode when the large joint spacing ratio is used. Pure plane sliding failure is observed when the slope models are gentle and low, while combination of plane and circular failures is observed when the slopes are steep and high.

6. DISCRETE ELEMENT ANALYSIS

Discrete element analyses are performed using UDEC (Itasca, 2004) to describe the stability conditions of the slope in the physical models. The discrete element models are constructed to represent various slope geometries and joint spacings as used in the physical model testing. The rock block model uses a density of $2,270 \text{ kg/m}^3$ which is equal to the density of Phu Phan sandstone. The bulk modulus and shear modulus of the sandstone are calculated from the elastic modulus and Poisson's ratio as 12.3 GPa and 3.8 GPa. The normal and shear joint stiffness values (K_n and K_s) for the smooth joint in Phu Phan sandstone determined by Suanprom (2009) are 10 GPa/m and 8 GPa/m, respectively. The joint friction angle and cohesion used in the simulations are 21° and 0.053 kPa. They are obtained from the tilt testing. All computer simulations assume plane stress condition. The dilatancy of the joints is assumed to be zero because the surfaces of the tested sandstone blocks are smooth and the cohesion is very low. The corner rounding and the minimum edge length are taken here as 0.001% and 0.002% because the tested sandstone blocks are cubical and rectangular blocks with sharp corners and flat surfaces.

Table 1. Summary of simulation parameters and results.

$S_H:S_V$	ψ_f (degrees)	H/S_H	ψ_p (degrees)	Failure Modes
1:2	33-39	7.8-12.5	23-25	Plane
		14.5-20.7	20-22	Plane/Circular
	40-52	3.5-8.6	23-25	Plane
1:3	58-69	10.2-24.2	16-22	Plane/Circular
		5.2-7.9	22-23	Plane
	40-46	10.3-24.4	15-20	Plane/Circular
1:4	52-57	4.4-18.8	23-27	Plane
		6.1-18.1	22-24	Plane
	62-68	20.8-26.4	19-20	Plane/Circular
1:4	32-36	5.2-10.6	22-23	Plane
		13.1-23.2	19-21	Plane/Circular
	44-52	5.3-21.0	23-26	Plane
	54-57	6.9-19.5	24-25	Plane
21.3-24.7		22-23	Plane/Circular	
		10.0-13.0	22-23	Plane
		17.0-21.0	21-22	Plane/Circular

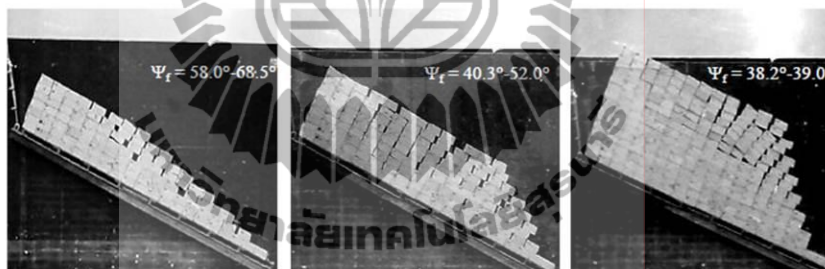
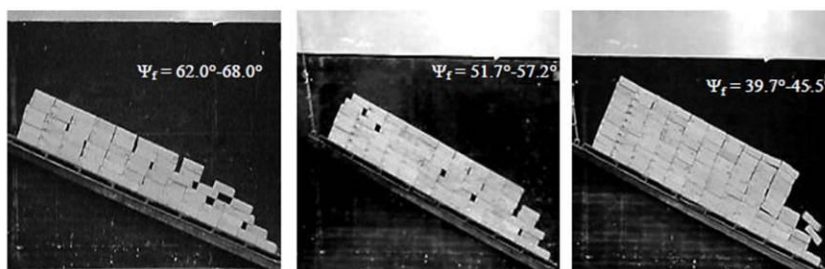
**Figure 3.** Some test results for various slope heights for $S_H:S_V = 1:2$.**Figure 4.** Some test results for various slope heights for $S_H:S_V = 1:3$.



Figure 5. Some test results for various slope heights for $S_H:S_V=1:4$.

Figure 6 compares the UDEC results with the physical model test results in form of the slope height ratio (H/S_H) as a function of sliding plane angle (ψ_p). The numerical results agree well with the physical model simulations. Two models of failure are observed from the UDEC results: pure plane sliding and combination of plane sliding and circular failure. The pure plane sliding mode is obtained from low slope heights with high joint spacing ratios. The combination mode occurs from high slopes with low joint spacing ratio. Under the same sliding plane angle the UDEC results tend to show higher slope height at failure. This is primarily because the rock blocks constructed in the UDEC model are perfectly shaped while small defects exist in the rock blocks used in the physical models. Both UDEC and physical models indicate that the slopes comprising large joint spacing ratio (e.g., $S_H/S_V = 1:4$) tend to fail by plane sliding mode while those with small joint spacing ratio (e.g., $S_H/S_V = 1:2$) fail under pure plane sliding and combination of plane sliding and circular failure. In addition pure plane sliding failure is observed when the slope models are gentle and low, while combination of plane and circular failures is observed when the slopes are steep and high.

Figures 7 and 8 compare the UDEC slope models with the physical slope models while the failure (sliding) is in progress.

Similar failure sequence is observed from the two methods of simulation. Failure starts near the slope faces and propagates back into the slope mass.

7. DETERMINISTIC METHOD

Assuming that the plane sliding mechanism follows the Coulomb criterion, the deterministic method uses an equation modified from Wyllie et al. (2004) and Kroeger (2000) to calculate the sliding plane angle as show below.

$$FS = \frac{c \cdot A + (W \cdot \cos \psi_p) \cdot \tan \phi}{W \cdot \sin \psi_p} \quad (2)$$

where c is cohesion of rock surface (equal to 0.053 kN/m^2), ϕ is friction angle (equal to 21 degrees), ψ_p is the inclined sliding plane, W is weight of sliding block, and A is the contact area of sliding surface.

$$W = \gamma_f \left[(1 - \cot \psi_f \cdot \tan \psi_p) (bH + \frac{1}{2} H^2 \cdot \cot \psi_f) + \frac{1}{2} b^2 (\tan \psi_s - \tan \psi_p) \right] \quad (3)$$

$$A = (H + b \tan \psi_s - z) \cos \psi_p \quad (4)$$

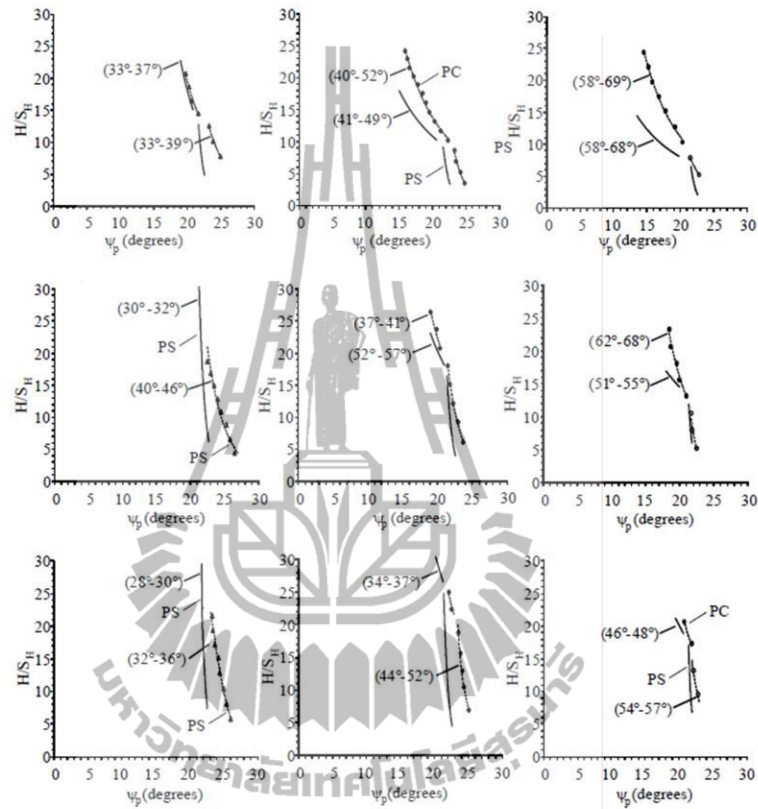


Figure 6. Comparisons between test results and numerical analysis for 4×8 cm blocks (top), 4×12 cm blocks (middle) and 4×16 cm blocks (bottom). PC and PS indicate combination of plane and circular failures and pure plane sliding, respectively.

$$b = H \sqrt{\cot \psi_f \cdot \cot \psi_p} - \cot \psi_f \quad (5)$$

$$z = H [1 - \cot \psi_f \cdot \tan \psi_p] + b [\tan \psi_s - \tan \psi_p] \quad (6)$$

where ψ_s is the inclined upper slope face, ψ_{f0} is the initial slope face angle, ψ_f is the slope face angle at failure ($\psi_f = \psi_{f0} + \psi_p$), γ_r is the unit

weight of rock (equal to 23.8×10^3 kN/m³ for Phu Phan sandstone), H is height of slope at failure, b is the tension crack location measured from the slope crest, and z is the vertical tension crack depth. The factor of safety of 1.0 is taken to represent the condition at which failure occurs in the slope models.

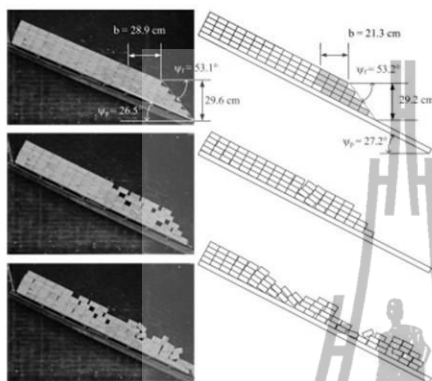


Figure 7. Comparisons of UDEC simulations with physical model tests for 4×8 cm block. The slope height is about 30 cm with slope face of 53 degrees.

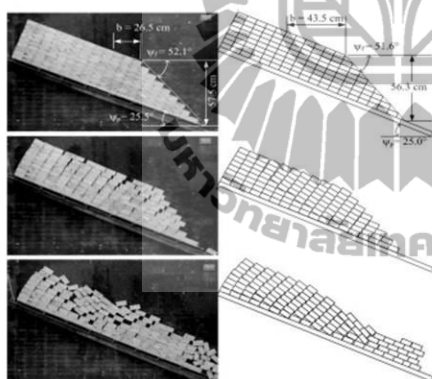


Figure 8. Comparisons of UDEC simulations with physical model tests for 4×8 cm block. The slope height is about 57 cm with slope face of 52 degrees.

Figure 9 compares the sliding angles obtained from the deterministic method with those of the physical model tests for the same slope geometry. Under the same sliding angle the deterministic method overestimates the

slope height at failure for the slopes fail by combination modes. It however slightly underestimates the slope height at failure for those fail by pure plane sliding. This behavior is clearly pronounced for the slopes with small joint spacing ratios. The results suggest that stability analysis using the deterministic method may not be conservative for jointed rock slopes.

8. DISCUSSIONS AND CONCLUSIONS

It is recognized that the joints simulated in the slope models here are very smooth and clean with low cohesion and friction angle, which may not truly represent most actual rock joints found in in-situ rock slopes. Nevertheless the comparisons of the test results with the deterministic solutions (by Hoek & Bray, 1981) and computer simulations (UDEC code) under the same test parameters (e.g., joint properties and slope characteristics) have revealed significant implications. The deterministic method and computer simulation over-estimate the sliding plane angles, particularly for the slope models with small joint spacings. This is probably due to the impacts of the block spacing, block shape and interaction forces between the discrete blocks in the sliding mass. This implies that stability analysis by assuming that the sliding mass is continuous as used by the deterministic method may not be conservative, particularly for slope masses with short-spaced joints compared to the slope height. Cast cement blocks with various degrees of pre-defined roughness on the surfaces.

9. ACKNOWLEDGEMENT

This research is funded by Suranaree University of Technology. Permission to publish this paper is gratefully acknowledged.

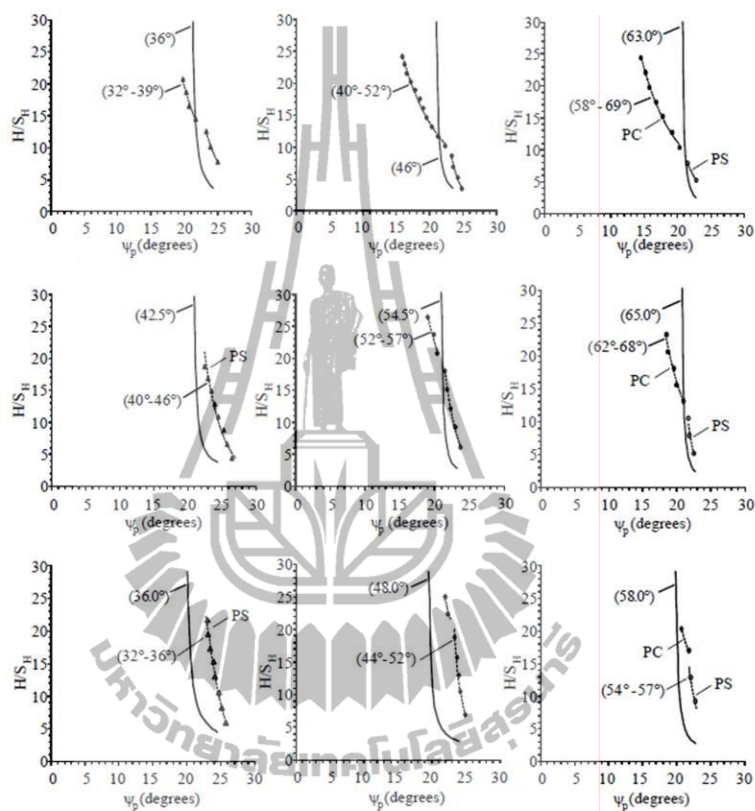


Figure 9. Comparisons between test results and deterministic method for 4×8 cm blocks, 4×12 cm blocks and 4×16 cm blocks. PC and PS indicate combination of plane and circular failures and pure plane sliding, respectively.

10. REFERENCES

- Bray, J.W. & Goodman, R.E., 1981. The theory of base friction models. *International Journal of Rock Mechanics and Mining Science and Geomechanics*, 18(6): 453-468.
- Goodman, R.E., 1976. *Models of geological engineering in discontinuous rock*. West Publishing Company, St Paul, Minnesota, USA.
- Hittinger, M., 1978. *Numerical analysis of toppling failures in jointed rock*. Ph.D. Thesis, University of California, Berkeley, USA.
- Hoek, E. & Bray, J.W., 1981. *Rock slope engineering*, 3rd edition, Institute of Mining and Metallurgy, London.

- Itasca, 2004. UDEC 4.0 GUI A Graphical User Interface for UDEC. Itasca Consulting Group Inc., Minneapolis, MN.
- Kim, Y.G. & Lee, H.K., 1992. Slope stability analysis in discontinuous rocks by base friction model test and its numerical analysis. Regional Symposium on Rock Slopes. Coal India Limited, India, pp. 195-201.
- Kroeger, E.B. 2000. Analysis of plane failures in compound slopes. *International Journal of Surface Mining, Reclamation and Environment* 14: 215-222.
- Lanaro, F., Jing, L., Stephansson, O. & Barla, G., 1997. D.E.M. Modeling of laboratory tests of block toppling. *International Journal of Rock Mechanics and Mining Sciences*, 34(3-4): 173.
- Pangpetch, P. & Fuenkajorn, K., 2007. Simulation of rock slope failure using physical model. In Proceedings of the First Thailand Symposium on Rock Mechanics. Suranaree University of Technology, Nakhon Ratchasima. pp. 227-243.
- Suanprom, 2009. Permeability testing of sheared fractures in sandstones. MS. Thesis, Geotechnology, Suranaree University of Technology. 78 pp.
- Teme, S.C., 1987. A kinematic modeling machine for rock slope studies. *International Journal of Mining and Geological Engineering*, 5: 75-81.
- Terzaghi, K., 1950. Mechanisms of landslides. In *Application of Geology to Engineering Practice*. Geol. Soc. of America, New York, Berkey, pp. 83-123.
- Wyllie, D.C., Mah, C.W. & Hoek, E. 2004. *Rock Slope Engineering: Civil and Mining*. The Institution of Mining and Metallurgy, London.



BIOGRAPHY

Miss. Matsee Kleepmek was born on October 10, 1987 in Chaing Mai province, Thailand. She received her Bachelor's Degree in Engineering (Geotechnology) from Suranaree University of Technology in 2010. For her post-graduate, she continued to study with a Master's degree in the Geological Engineering Program, Institute of Engineering, Suranaree university of Technology. During graduation, 2010-2012, she was a part time worker in position of research assistant at the Geomechanics Research Unit, Institute of Engineering, Suranaree University of Technology. She has published two technical papers related to rock mechanics as; In 2011, **“Physical model simulation of jointed rock slopes”** published in the Proceedings of the Third Thailand Symposium on Rock Mechanics, Cha-Am Beach, Thailand; In 2011 **“Simulation of jointed rock slope using physical model”** in the Proceeding of EIT-Japan Symposium 2011 on Human Security Engineering, Bangkok, Thailand.